



Eurodelta multi-model simulated and observed PM trends in Europe in the period of 1990-2010

Svetlana Tsyro¹, Wenche Aas², Augustin Colette³, Camilla Andersson⁴, Bertrand Bessagnet^{3,†}, Giancarlo Ciarelli³, Florian Couvidat³, Kees Cuvelier⁵, Astrid Manders⁶, Kathleen Mar⁷, Mihaela Mircea⁸, Noelia Otero⁷, Maria-Teresa Pay⁹, Valentin Raffort¹⁰, Yelva Roustan¹⁰, Mark R. Theobald¹¹, Marta G. Vivanco¹¹, Hilde Fagerli¹, Peter Wind^{1,12}, Gino Briganti⁸, Andrea Cappelletti⁸, Massimo D'Isidoro⁸, and Mario Adani⁸

¹Norwegian Meteorological Institute, NO-0313, Oslo, Norway

²Norwegian Institute for Air Research (NILU), Box 100, 2027 Kjeller, Norway

⁴INERIS, National Institute for Industrial Environment and Risks, Parc Technologique ALATA, 60550, Verneuil-en-Halatte, France

³Swedish Meteorological and Hydrological Institute, 60176 Norrköping, Sweden

⁵ex European Commission, Joint Research Centre (JRC), Ispra, Italy

⁶TNO, Dept. Climate, Air and Sustainability, P.O. Box 80015, 3508 TA Utrecht, the Netherlands

⁷Institute for Advanced Sustainability Studies, Potsdam, Germany

⁸ENEA, Italian National Agency for New Technologies, Energy and Sustainable Economic Development Via Martiri di Monte Sole 4, 40129 Bologna, Italy

⁹BSC, Barcelona Supercomputing Center, Centro Nacional de Supercomputaci3n, Nexus II Building, Jordi Girona, 29, 08034 Barcelona, Spain

¹⁰CEREA, École des Ponts, EDF R&D, Île-de-France, France

¹¹CIEMAT, Atmospheric Pollution Unit, Avda. Complutense, 22, 28040 Madrid, Spain

¹²Faculty of Science and Technology, University of Tromsø, Tromsø, Norway

[†]Now at European Commission, Joint Research Centre (JRC), Ispra, Italy

Correspondence: Svetlana Tsyro (svetlana.tsyro@met.no)

Abstract.

The Eurodelta-Trends multi-model experiment, aimed to assess the efficiency of emission mitigation measures in improving air quality in Europe during 1990-2010, was designed to answer a series of questions regarding European pollution trends. i.e. were there significant trends detected by observations? do the models manage to reproduce observed trends? how close is the agreement between the models and how large are the deviations from observations? In this paper, we address these issues with respect to PM pollution. An in-depth trend analysis has been performed for PM₁₀ and PM_{2.5} for the period of 2000-2010, based on results from six chemical transport models and observational data from the EMEP (Cooperative Programme for Monitoring and Evaluation of the Long-range Transmission of Air Pollutants in Europe) monitoring network. Given harmonization of set up and main input data, the differences in model results should mainly result from differences in the process formulations within the models themselves, and the spread in the models simulated trends could be regarded as an indicator for modelling uncertainty.



The model ensemble simulations indicate overall decreasing trends in PM_{10} and $PM_{2.5}$, with reduction by between 2 and 6 $\mu g m^{-3} m^{-3}$ (or between 10 and 30%) from 2000 to 2010. Compared to $PM_{2.5}$, relative PM_{10} trends are weaker due to large inter-annual variability of natural coarse PM within the former. The changes in the concentrations of PM individual components are in general consistent with emission reductions. There is a reasonable agreement in PM trends estimated by the individual models, with the inter-model variability below 30-40% over most of Europe, increasing to 50-60% in northern and eastern parts of EDT domain.

Averaged over measurement sites (26 for PM_{10} and 13 for $PM_{2.5}$), the mean ensemble simulated trends are -0.24 and -0.22 $\mu g m^{-3} year^{-1}$ for PM_{10} and $PM_{2.5}$, which are somewhat weaker than the observed trends of -0.35 and -0.40 $\mu g m^{-3} year^{-1}$, respectively, partly due to models underestimation of PM concentrations. The correspondence is better in relative PM_{10} and $PM_{2.5}$ trends, which are -1.7 and -2.0 % $year^{-1}$ from the model ensemble and -2.1 and -2.9 % $year^{-1}$ from the observations, respectively. The observations identify significant trends for PM_{10} at 56 % of the sites and for $PM_{2.5}$ at 36% of the sites, which is somewhat less than the fractions of significant modelled trends. Further, we find somewhat smaller spatial variability of modelled PM trends with respect to the observed ones across Europe and also within individual countries.

The strongest decreasing PM trends and the largest number of sites with significant trends is found for the summer season, according to both the model ensemble and observations. The winter PM trends are very weak and mostly insignificant. One important reason for that is the very modest reductions and even increases in the emissions of primary PM from residential heating in winter. It should be kept in mind that all findings regarding modeled versus observed PM trends are limited to the regions where the sites are located.

The analysis reveals a considerable variability of the role of the individual aerosols in PM_{10} trends across European countries. The multi-model simulations, supported by available observations, point to decreases in SO_4^{2-} concentrations playing an overall dominant role. Also, we see relatively large contributions of the trends of NH_4^+ and NO_3^- to PM_{10} decreasing trends in Germany, Denmark, Poland and the Po Valley, while the reductions of primary PM emissions appears to be a dominant factor in bringing down PM_{10} in France, Norway, Portugal, Greece and parts of the UK and Russia.

Further discussions are given with respect to emission uncertainties and the effect of inter-annual meteorological variability on the trend analysis.

1 Introduction

The Convention on Long-range Transboundary Air Pollution (LRTAP), signed in 1979, addresses some of the major environmental problems of the UNECE region through scientific collaboration and policy negotiation (UNECE, 2004). Parties develop policies and strategies to combat the release of pollutants in the atmosphere through exchanges of information, consultation, research and monitoring. During the 1980s, 1990s and 2000s, the concentrations of particulate matter (PM) were decreasing due to the decrease of secondary inorganic aerosols (SIA) as a result of the reductions of the emissions of their gaseous precursors in order to address the acidification and eutrophication problems (Fagerli and Aas (2008), Aas et al. (2019)), mainly of SO_x due to the 1st and 2nd Sulphur Protocols, and also NO_x and NH_3 in line with the 1999 Gothenburg Protocol to Abate Acidifi-



cation, Eutrophication and Ground-level Ozone (UNECE, 2004). The emissions of primary PM were not then regulated, but still were decreasing as a side-effect of the reductions of gaseous pollutants. In the end of 1990s, the issue of adverse effects of particulate pollution on human health came into focus, and in 2012, emissions of primary PM_{2.5} were included in the revised
50 Gothenburg Protocol, stating that fine particulate matter is "the pollutant whose ambient air concentrations notoriously exceed air quality standards throughout Europe".

The Eurodelta-Trends (EDT) multi-model experiment, involving eight chemical transport models (CTMs), has been designed in order to better understand the evolution of air pollution and its drivers since the early 1990s. The main objective of the experiment is to assess the efficiency of air pollutant emissions mitigation measures in improving regional scale air quality
55 in Europe. The multi-model trend analysis is a contribution to the assessment of the evolution of air pollution in the EMEP region over the 1990-2012 period coordinated by the Task Force on Monitoring and Modelling (TFMM) of EMEP (Cooperative Programme for Monitoring and Evaluation of the Long-range Transmission of Air Pollutants in Europe). The synthesis of the observational and modelling evidences of atmospheric composition and deposition change in response to actions taken by to control emissions were given in Colette et al. (2016).

A number of studies of European (and global) PM trends for the 1990s and 2000s have been performed and published last years. Some studies analysed observed PM trends (e.g. Guerreiro et al. (2014), Barmadimos et al. (2012), Cusack et al. (2012), EEA (2009), Crippa et al. (2016)), including those derived from remote sensing observations (Van Donkelaar et al., 2015), whereas a limited number of analysis also included model simulations (e.g. Colette et al. (2011), Mortier et al. (2020), Colette et al. (2021), Myhre et al. (2017)). Rather a large spread of observed and modelled PM trends, both decreasing and
65 increasing, has been reported for the period between 1998-2002 and 2008-2014. Analysis of EMEP observed 2002-2012 trends, also performed under TFMM coordination by Colette et al. (2016), reported the median trends of $-0.35 \mu\text{g m}^{-3} \text{yr}^{-1}$ PM₁₀ and -0.29 for PM_{2.5}, resulting in the reduction over the period by -29 and -31%, respectively, with 95% probability. As we discuss in this paper, being overall consistent with the earlier trend assessments, the results presented here are believed to be more robust as they rely on a multi-modelling approach.

The main science and policy questions addressed by the EDT modelling experiment are formulated in Colette et al. (2017a), in which also the design and technical specifics of the modelling exercise are described in detail. The studied period covered a 21-year time-span, from 1990 through 2010, and in total eight regional CTMs have participated. In this paper, we present the results of trend study with respect to Particulate Matter (PM) pollution in Europe. An in-depth trend analysis for PM₁₀ and PM_{2.5} has been performed for a period of 2000-2010, based on multi-model simulations and EMEP monitoring data.
75 The shorter period for PM trend study than the 1990-2010 EDT period was chosen due to the lack of appropriate PM₁₀ and PM_{2.5} observations prior 2000. Not all of the eight EDT models had resources to perform all simulations, therefore trend analysis presented in this work are based on the results from six of the models. Also, multi-model simulated PM trends during the whole 1990-2010 period are briefly discussed here. The strength of the presented assessment is that the model ensemble simulated PM trends represent more a robust estimate as compared to either of the individual models, while the multi-model
80 simulations allowed us investigating into the variability of modelled results, obtained under the controlled setup. Finally, the model simulations allow interpreting PM trends in term of the trends in the individual aerosols. This is a valuable contribution



to better understanding the correspondence between emission changes and PM concentration levels across Europe, given the lack of observational data on PM chemical composition.

The paper is structured as follows: Section 2 describes the methods used, including brief information on the models, runs' setup, observations and trend calculations; Section 3 summarizes model evaluation with respect to PM; Section 4 presents emission trends; Section 5 is dedicated to PM 2000-2010 trend analysis for the whole Europe and for set of measurement sites, discusses PM seasonal trends and the relative contribution of PM components; in Section 6 we show modelled PM trends for the 1990-2010 period. Further discussion of the result is given in Section (including emission uncertainties and effect of meteorological variability); and finally the main outcomes and findings can be found in Section 8.

2 Methods

2.1 Models, runs setup

The trend analysis is based on the results from six of the EDT models, namely the ones which provided a complete series of 2000-2010 simulations. Those models are CHIMERE (CHIM), EMEP MSC-W (EMEP), LOTOS-EUROS (LOTO), MATCH, MINNI and Polair3D (POLR). These models, with the exception of POLR, also performed simulations for the 1990-1999 period.

A comprehensive description of the models participated in the Eurodelta-Trends experiment, the simulations setup, input data and the overview of the computations performed is given in Colette et al. (2017a).

Briefly, the setup and input data for the EDT simulations were harmonized as far as possible. The models performed the simulations on the same grid with a resolution of $0.25^\circ \times 0.4^\circ$ in latitude-longitude coordinates. The simulations were driven by the same meteorological input from hindcast simulations of the CORDEX project (Jacob et al. (2014) and Stegehuis et al. (2015)) using the WRF (Weather Research and Forecast) model (Skamarock et al., 2005) at $0.44^\circ \times 0.44^\circ$ resolution and using boundary conditions from ERA-Interim reanalysis (Dee et al., 2011). The exceptions were LOTO and MATCH, which used ERA-Interim reanalysis downscaled respectively by RACMO2 (Van Meijgaard et al., 2012) and HIRLAM (Dahlgren et al., 2016).

Furthermore, the models used the same gridded anthropogenic emissions of SO_2 , NO_x , NH_3 , NMVOC, CO, PM_{10} and $\text{PM}_{2.5}$ (Terrenoire et al. (2015) and Bessagnet et al. (2016)). The national emissions were based on the ECLIPSE_V5 dataset, constructed by the Greenhouse Gasses and Air pollution INteraction and Synergies (GAINS) model (Amann et al. (2011), Amann (2012), Klimont et al. (2016), Klimont et al. (2017)) and provided in SNAP (Selected Nomenclature for reporting of Air Pollutants) sectors. Spatial distribution of the national sectoral emissions, performed by INERIS applying auxiliary information which included road maps (for SNAP sector 7), shipping routes (for SNAP 8) and population density (for SNAP 2), the European Pollutant Release and Transfer Register (for SNAP 1, 3, 4), TNO-MACC inventory for NH_3 emissions, as well as bottom-up emission inventories for the UK and France (see details in Colette et al. (2017a) and references therein). Time changes in the spatial distribution was accounted for only for industrial emissions. Vertical distribution and temporal profiles for the emissions used in the model simulations were those used in the EMEP model standard setup (Simpson et al.,



115 2012). The ECLIPSE_V5 emissions were available for the years 1990, 1995, 2000, 2005 and 2010, while for the intermediate years the emissions were derived through linear interpolations (Colette et al., 2017a).

At a rather late stage of the experiment, an error was detected in the emissions of primary particulate matter from international shipping, Russia and North Africa for the period 1991-1999. Since this error was identified late in the analysis process it was not possible to re-run the simulations with corrected emissions. The additional analysis of the impact of this error carried out
120 with the CHIMERE model showed that these errors are relatively small compared with the overall uncertainty of the model estimates and the uncertainty of the observations (see more details in Theobald et al. (2019)). Nevertheless, the main focus of this paper is on the analysis of PM trends in the course of the 2000s, i.e. the period for which model results were not affected by the emission error.

Natural emissions of biogenic VOCs, soil NO_x, sea salt and mineral dust were calculated/prescribed within the models indi-
125 vidually. Online computations of windblown dust from erodible soils were performed by EMEP, LOTO and MINNI, whereas the other models included solely mineral dust from boundary conditions. Forest fire emission were not included in the EDT simulations; and SO₂ emissions from Italian volcanoes were only included in the EMEP and MATCH models. Finally, the common boundary conditions, provided by the EMEP group were based mainly on a climatology of observational data (Simpson et al., 2012). Given harmonization of set up and main input data (with a few exceptions), the differences in model results
130 should mainly result from differences in the process formulations within the models themselves.

2.2 Observations

The observations collected at the EMEP monitoring network are annually reported to the Chemical Coordinating Centre of EMEP (Tørseth et al., 2012). All submitted observational data, after routine quality and consistency control, are available in EBAS (<http://ebas.nilu.no>). Most of the sites used a gravimetric method for both size fractions, though some used monitors.
135 The same methods are used during the whole period. Details about site locations and applied methods are found in Table A1.

As documented in Colette et al. (2016), the selection criteria for sites included in the trend analysis were: i) the data capture should be at least 75 % for a specific year to be counted and ii) the number of these counted years should be at least 75 % of the total number of years in the period, and had undergone visual screening tests. The datasets used in this work include yearly measurements of observed trends from respectively 26 and 13 sites of PM₁₀ and PM_{2.5} for the period 2000-2010 (Table A1).
140 Among those 'trend-sites', PM₁₀ observations are available for all eleven years of the 2000-2010 period at 16 sites, and only at 4 site for PM_{2.5}. In particular, the observational data is missing at rather many sites for the first trend period year, namely 2000. For the calculations of trend slopes and for models evaluation, only available observational data is used (the number of valid years used in those statistical calculations is given in Table A1). For time-series of annual and seasonal mean PM₁₀ and PM_{2.5}, averaged over all trend sites (Figures 4 and 8), a gap filling of the missing years was undertaken, to ensure that the
145 same sites were used through the years 2000-2010. The gap fillings were done by averaging between the adjacent years. For the first (2000) or the last (2010) year, the missing data were filled with values from the next or previous year.



2.3 Trend calculation

The Mann Kendall (MK) method (Mann (1945), Kendall (1975)) has been applied to both modelling results and observed data for identification of significant trends. The linear trends have been calculated using the Theil-Sen slope method (known to be robust to outliers), applying the probability level of 95% as a threshold for trend significance. The trend calculation method used here is consistent with that in trend assessment reported in Colette et al. (2016). In addition to absolute concentration trends, relative trends have been calculated using an estimated concentration at the start of the period (i.e. the year of 2000) as reference (see Appendix A3 in Colette et al., 2016). This concentration value corresponds to PM concentration in 2000 according to the trend line, and is considered to be less sensitive to inter-annual variability than the actual observed or modelled ones.

A synthetic testing of the efficiency of MK methodology to identify significant trends and estimate Sen's slopes has been performed (S. Solberg, *personal comm.*, https://wiki.met.no/_media/emep/emep-experts/mannkendall_note.pdf). It showed that the chance that the MK method detects the long-term trend decreased for shorter data-series, large natural variability and relatively weak trends. Further, it was found that gap-filling of data for 1-2 years did not appear to impact MK analysis results. The aforementioned document also demonstrates that taking into consideration (averaging) significant trends only would overestimate mean absolute trends.

3 Models evaluation

Model simulated PM₁₀ and PM_{2.5} have been evaluated against observations at the trend-sites (26 and 13 respectively) for the years from 2000 through 2010, and averaged over the measurement sites performance statistics in terms of annual mean bias and spatial correlations are summarized in Figure 1 and Tables A2 and A3 (Appendix A).

Figure 1 shows the relative biases (in %) for the individual model and the ensemble mean. The modelled PM₁₀ and PM_{2.5} tend to be biased low compared to the observations (marked by blue colours of different intensity). On average, the model ensemble underestimates annual mean PM₁₀ by 12% and PM_{2.5} by 14% over the period 2000-2010 (rather different biases for 2000 are due to fewer sites with data). PM₁₀ mean relative biases for the individual models are in a range of 5-11 %, that is somewhat smaller than their biases of 5-20 % for PM_{2.5} (with POLR standing out with PM₁₀ bias of -31% as erroneously simulated coarse sea salt had to be excluded).

Furthermore, we find a quite moderate year-to-year variability of the model ensemble bias, namely between -7 and -18% for PM₁₀ and between -2 and -20% for PM_{2.5}. This robustness in PM simulation also applies to the individual models, i.e. the inter-annual bias variations are mostly within 5% (up to 10%). The consistency in terms of bias can be noticed between the models (e.g. smaller underestimation of PM₁₀ for 2000, 2001, 2007, 2008 and 2009, whilst slightly larger underestimation for the years 2003, 2006 and 2010, characterised by elevated PM levels).

The average annual coefficients of spatial correlation are 0.54 (0.41 - 0.58) for PM₁₀ and 0.65 (0.58-0.72) for PM_{2.5}. Similar to model biases, the correlation varies only moderately between the years and the models (Tables A2 and A3). Models'



evaluation for the individual aerosol components and their gaseous precursors can be found in the other EDT publications (e.g.
180 Ciarelli et al., 2019; Theobald et al., 2019).

4 Emission trends

The graphs in Figure A1 present the changes in European annual emissions, used in this work. The total emissions of aerosol
gaseous precursors SO_2 , NO_x and NH_3 and primary fine and coarse PM ($\text{PM}_{2.5}$ and $\text{PM}_{10-2.5}$) are shown for the whole period
of EDT study, i.e. 1990-2010. The total emissions of all pollutants decrease during this period, although at different rates. From
185 1990 to 2010, the greatest decrease by 69% is in SO_2 emissions, following by NO_x emissions which are decreased by 39%.
The reduction in NH_3 emissions is rather moderate 15%. Quite considerable decrease is seen in primary PM emissions, which
go down by 67 and 47% for coarse PM and $\text{PM}_{2.5}$ respectively.

During the period of 2000-2010, which is in a focus of this publication, the total emission decreases are: 37% for SO_2 , 17%
for NO_x , 6% for NH_3 , 27% for $\text{PM}_{2.5}$, 36% for coarse PM, 33% for NMVOC. For EU area, where the measurement sites with
190 PM observations available for the trend analysis are located, SO_2 is reduced by 24%, NO_x by 22%, NH_3 , $\text{PM}_{2.5}$ and coarse
PM by 10% during the same period.

Further details on emission changes across the EDT domain are provided in Figure A2, which shows the maps with annual
mean trends in the emissions of primary PM and their gaseous precursors during 2000-2010 and 1990-2010. During the period
of our attention 2000-2010, the emissions of SO_2 and NO_x go down in all countries, but there are many hot-spots with upward
195 trends (also in some Eastern and south-Eastern countries for NO_x). The negative trends of SO_2 emissions are 3-7% per year in
most countries, exceeding 7%/yr in Italy, Hungary, Portugal, Ireland and parts of Sweden and Finland (below 3%/yr in Western
Balkan, Norway and Russia). NO_x emissions show a reduction of 3-5%/yr in Central Europe and Italy, going up 5-7%/yr
and above in Sweden, some spots in Finland, Denmark, the UK and Portugal. NO_x decreases less (by 1-3 %/yr) in Norway,
parts of Spain and Eastern Europe, and increases by 1-3 %/yr in Russia, Belarus, parts of Poland. SO_2 and NO_x emissions
200 from international shipping decrease in the North Atlantic and the Baltic Sea, but increase in the Mediterranean Sea. Also
 NH_3 emissions show negative trends in most of the domain, with decrease by 0.5-3%/yr in most of Europe (by 3-5 %/yr in
Denmark), but they remain nearly unchanged in Scandinavia and even increase by 1-3%/yr in Belarus, Lithuania, Estonia and
Bosnia and Herzegovina and by (0.5-1.5%/yr) in Poland.

During 2000-2010, $\text{PM}_{2.5}$ emissions show downward trends in Central Europe and Norway (-3-5%/yr) and in the rest of
205 Eastern Europe, Spain and Scandinavia (-1-3%/yr), while they go up (by 1-4%/yr) in Italy, Poland, Denmark, Bosnia and
Herzegovina, Serbia, Moldova and Turkey. Finally, the largest decrease in coarse PM emissions is in Portugal (by (3-5)%/yr),
and in the UK, Belgium and parts of Central and South-Eastern Europe (by (1-5)%/yr), but there are hot-spots with 1-4%/yr
emission increase in the latter areas. PM coarse emissions also increase in parts of Scandinavia and Finland, in the Baltic
countries and in Russia (by 1-4%/yr), whereas they change little elsewhere.



210 5 PM trends for the period 2000-2010

5.1 Modelled and observed European trends

Figure 2 shows the maps of mean annual trends (Sen's slopes) of PM_{10} and $\text{PM}_{2.5}$ over Europe for the period of 2000-2010, calculated by the ensemble of six models (mean of EMEP, CHIM, LOTO, MINNI, MATCH and POLR) and observed at EMEP sites. The trends are presented in terms of absolute (in $\mu\text{g m}^{-3} \text{yr}^{-1}$) and relative to the starting year of 2000 ($\%\text{yr}^{-1}$) annual changes. Significant trends are represented by coloured contour maps (modelled) and triangles (observed), whereas the insignificant trends are shown as grey areas and circles respectively.

The model results over the simulation domain and the observations at the trend-sites show overall decreasing trends of PM_{10} and $\text{PM}_{2.5}$ levels between 2000 and 2010. The modelled mean decreasing trends vary over the studied domain from below $0.1 \mu\text{g m}^{-3} \text{yr}^{-1}$ in northern Europe to $0.1\text{-}0.3 \mu\text{g m}^{-3} \text{yr}^{-1}$ in the eastern parts, and to $0.3\text{-}0.5 \mu\text{g m}^{-3} \text{yr}^{-1}$ in central Europe and most of the UK, with $\text{PM}_{2.5}$ downward trends being just slightly smaller than those for PM_{10} . Starting from the concentration levels in 2000, the mean relative decreasing trends range mostly from 0.1 to $0.3 \%\text{yr}^{-1}$ for PM_{10} and $\text{PM}_{2.5}$. Compared to the distribution of absolute trends, steeper slopes of relative decreasing trends are also seen in the southern parts of Fennoscandia in addition to Central Europe and the UK.

The 6-model simulated mean trends are in general comparable to the observed ones, still some discrepancies are seen in their geographical distribution. For instance, quite strong decreasing trends for PM_{10} and for $\text{PM}_{2.5}$ are observed at three of the Spanish sites, while the model ensemble does not practically indicate any significant trends over Spain. It should be noted that the models do calculate negative PM trends for the Spanish sites (as seen in A7), but due to considerable inter-annual variability most of them are not identified as significant. Furthermore, the models calculated strongest decreasing trends of $0.5\text{-}0.7 \mu\text{g m}^{-3} \text{yr}^{-1}$ for PM_{10} and $\text{PM}_{2.5}$ in Portugal and Benelux, but no measurements were available to validate the modelled results. For Germany, the slopes of observed trends are similar or somewhat lower than the modelled, but unlike the model results, none of the observed trends was identified as significant. In the next sections, the trends at the individual monitoring sites will be considered more closely.

Figure 3 illustrates the inter-model variability in PM trend slopes, showing the Coefficient of Variability (COV) of the trends simulated by the individual models relative to the ensemble mean ($\text{STD}/\text{ensemble mean}$) for PM_{10} and $\text{PM}_{2.5}$. The COV is somewhat larger for the modelled PM_{10} trends compared to those for $\text{PM}_{2.5}$. This reflects larger uncertainties in modelling of the coarse fraction of PM, which is mostly due to natural origin. The lowest spread in the modelled trends (below 20%) appears in Central Europe (Germany, Czech Republic), and also parts of Spain, northern regions of Italy and in the very south of Scandinavia for $\text{PM}_{2.5}$. Those regions correspond with the strongest simulated PM trends. Otherwise, the COV is 20-40% over most of Europe, increasing to 40-60 % in Poland, western and northern Fennoscandia, the Baltic countries and parts of Russia, where the modelled trends are relatively low or insignificant.

The maps with annual mean PM_{10} and $\text{PM}_{2.5}$ trend slopes calculated by the individual models are provided in the Appendix. Figures A3 and A4 show the Sen's slopes of PM_{10} and $\text{PM}_{2.5}$ simulated by the six models and the observed trends for the period of 2000-2010. The significant modeled slopes are in general quite close to each other, indicating decreasing from 2000



to 2010 trends. Also the spatial variability of the Sen's slopes in the individual models' results shows much similarity, with the
 245 strongest decreasing trends identified in Central Europe (in particular in the Benelux countries and Germany). The EMEP and
 LOTOS calculated respectively the largest and the weakest negative mean trend slopes, as well as the largest and the smallest
 fraction of the modelling domain with significant PM trends, namely 45 % and 57 % grid-cells according to EMEP and 17
 and 38 % according to LOTOS for respectively PM_{10} and $PM_{2.5}$, with the results from the other for models lie between those
 values.

250 Relative to the year 2000, all the models simulate stronger trends for $PM_{2.5}$ compared to PM_{10} , as seen in Figures A5
 and A6. This is to be expected as the natural contribution, which is strongly meteorology dependent, is greater in PM_{10} .
 The distribution patterns of relative trends from the models are in general similar to those for corresponding absolute trends.
 However, there is a difference between the models in the locations of their strongest simulated relative trends, namely in Central
 Europe (e.g. EMEP, MINNI, POLR) or in Northern Europe (e.g. CHIM, LOTOS, MATCH). The fraction of the EDT domain
 255 with significant PM trends simulated with the individual models ranges from 17 (LOTO) to 45 (EMEP) % for PM_{10} and from
 38 (LOTO and MINNI) to 57 (EMEP) % for $PM_{2.5}$.

Figure 4 presents observed and modelled annual mean series of PM_{10} and $PM_{2.5}$ at the trend-sites for the period 2000-
 2010. Shown are the mean values from the 6-model ensemble (dotted curves in Fig. 4a) and from the individual models' results
 (Fig. 4b and c). Note that for those time series, the gap filling of the missing years in observational data described in section
 260 2.2 was applied.

Although they are an underestimation with respect to the observations, the annual mean concentrations of PM_{10} and $PM_{2.5}$
 from the 6-model ensemble follow the observed year-to-year PM variations well, with a peak in 2003 and a smaller one in
 2006 (the years with heatwave occurrences, which facilitated enhanced photo-chemical formation of sulphate and secondary
 organic aerosols and inhibited aerosol wet removal). Furthermore, the observations show a trend stagnation for PM_{10} and
 265 increase of $PM_{2.5}$ towards the end of the period at the sites considered. This is not reproduced accurately by the models. A
 look at the individual sites reveals that the observed increase is the result of $PM_{2.5}$ going up from 2008/2009 to 2010 at 7
 out of 13 sites. According to assessments of PM pollution in 2009 and 2010, presented in EMEP Status Reports 4/2011 and
 4/2012 (www.emep.int), about half of the sites with PM measurements reported an increase in annual mean PM_{10} and $PM_{2.5}$
 with respect to the year before. As documented in those reports, a 3-4 % decrease per year of PM_{10} was registered between
 270 2008 and 2010, whereas average $PM_{2.5}$ levels were similar in 2008 and 2009 and increased by 4% in 2010, averaged over all
 sites with PM data. However, large variations between monitoring sites were observed. For instance, enhanced annual mean
 PM_{10} , and particularly $PM_{2.5}$ levels, were reported for 2010 at Austrian, German, Swiss, and Finnish sites, which are among
 the trend-sites included in the present trend analysis. The major reason for elevated annual PM levels is often the occurrence
 of winter pollution episodes (caused by stagnant conditions within a very low boundary layer and exacerbated by enhanced
 275 emissions from domestic heating), which are not always accurately modelled due to either an overestimation of mixing layer
 height by relatively coarse vertical resolution or/and underestimation in the emission input data.

In general, the EDT model ensemble reproduces the observed annual 2000-2010 series of PM at the trend sites quite well,
 showing a high correlation of 0.95 for both PM_{10} and $PM_{2.5}$. Overall, the ensemble simulated PM_{10} and $PM_{2.5}$ concentrations



are lower than observed values by 31 and 19 % respectively (a greater bias for PM_{10} is partly caused by the POLR model - see
 280 below). A fairly good correspondence with respect to PM year-to-year changes is seen in Figures 4 (b, c) for the individual
 models compared with observations (with the exception of PM_{10} concentrations from POLR having a low bias because the
 contribution from coarse sea salt was not accounted for). Some deviations of LOTO's results for 2003 and 2006 are probably
 due to a different meteorological driver used in the model runs (LOTOS-EUROS was driven by ERA-interim downscaled
 by RACMO2 Colette et al., 2017a)). The correlation between the modelled and measured series of annual mean PM_{10} and
 285 $PM_{2.5}$ is high, with the following correlation coefficients: 0.96 and 0.93 for CHIM, 0.93 and 0.93 for EMEP, 0.77 and 0.85 for
 LOTO, 0.93 and 0.90 for MATCH, 0.93 and 0.88 for MINNI, and 0.70 and 0.87 for POLR, for PM_{10} and $PM_{2.5}$ respectively.
 These results give credibility to the results of the models and their ability to accurately simulate the changes in the PM levels
 due to emission changes, as well as represent the inter-annual variability due to meteorological conditions. These results also
 show that the model ensemble correlates better with the observations than the individual models when both PM_{10} and $PM_{2.5}$
 290 annual series are considered.

Linear trends for PM_{10} and $PM_{2.5}$ from the 6-model ensemble and observational data are represented by grey lines in Figure
 4a. Averaged over the sites, the mean ensemble simulated trends are $-0.24 \mu\text{g m}^{-3} \text{ year}^{-1}$ for PM_{10} and $-0.21 \mu\text{g m}^{-3} \text{ year}^{-1}$
 for $PM_{2.5}$. These are smaller compared with the observed -0.35 and $-0.40 \mu\text{g m}^{-3} \text{ year}^{-1}$, respectively, but can be anticipated
 given models' underestimation of PM concentrations. The correspondence between model results and observations is better in
 295 terms of relative 2000-2010 trends, which are -1.7 and -2.0% year^{-1} from the model ensemble and -2.1 and -2.9% year^{-1}
 from the observations, for PM_{10} and $PM_{2.5}$ respectively.

5.2 PM trends at the individual sites

Figure 5 presents observed and simulated (by the 6-model ensemble) PM_{10} and $PM_{2.5}$ trend slopes for each site for the
 period 2000-2010. The sites at which significant trends were observed are marked with a star. The modelled significant and
 300 insignificant trends are represented respectively by dark and light blue bars.

The observed and ensemble-modelled PM_{10} and $PM_{2.5}$ trends at all sites are decreasing. Figure 5 shows quite a large vari-
 ability of observed trends in mean concentrations, ranging between -0.08 and $-0.88 \mu\text{g m}^{-3} \text{ year}^{-1}$ for PM_{10} and between
 -0.05 and $-1.5 \mu\text{g m}^{-3} \text{ year}^{-1}$ for $PM_{2.5}$. Compared with the observations, ensemble-modelled trend slopes show less vari-
 ability across the sites: the Standard Deviations are 0.09 and $0.10 \mu\text{g m}^{-3} \text{ year}^{-1}$ versus 0.23 and $0.38 \mu\text{g m}^{-3} \text{ year}^{-1}$ in the
 305 observations for PM_{10} and $PM_{2.5}$ respectively (Table 1). The modelled trends are mostly within $-0.5 \mu\text{g m}^{-3} \text{ year}^{-1}$, and
 rather poorly correlated with the observations between the trend sites.

The strongest negative PM_{10} trends were observed at three of the Spanish sites and one Austrian site (with decreases greater
 than $0.7 \mu\text{g m}^{-3} \text{ year}^{-1}$), while the weakest (and mostly non-significant) trends were registered at British, Norwegian and some
 German sites (below $-0.15 \mu\text{g m}^{-3} \text{ year}^{-1}$). The strongest significant PM_{10} decreasing trend slopes were modelled for German
 310 and some other sites in Central Europe. For most of the Spanish sites, the model ensemble simulated PM decrease by 0.2 - 0.3
 $\mu\text{g m}^{-3} \text{ year}^{-1}$, but the trends were classified as insignificant. In general, we see a similar pattern in the results for $PM_{2.5}$,



with the exception that the strongest trend was both observed ($-1.5 \mu\text{g m}^{-3} \text{ year}^{-1}$) and modelled ($-0.4 \mu\text{g m}^{-3} \text{ year}^{-1}$) for Ispra (IT0004) in the Po Valley.

The observed relative trends range from -0.5 to -4.5 \%year^{-1} for PM_{10} and from -0.5 to -5.2 \%year^{-1} for $\text{PM}_{2.5}$ (Figure 6).
 315 Also in this case, ensemble-simulated relative trends show less variability, with values between -1.0 and -2.5 \%year^{-1} . The strongest negative PM_{10} trends (with rates of decrease greater than $-3.5 \text{ \% year}^{-1}$) were observed at three of the Spanish sites and the Swedish one, whereas the weakest and mostly non-significant trends (under -1 \% year^{-1}) were registered at the British and some German sites.

All in all, the observations show significant PM_{10} trends at 14 out of 26 sites and significant $\text{PM}_{2.5}$ trends at only 5 out
 320 of 13 sites. A closer look at PM_{10} and $\text{PM}_{2.5}$ annual series at the individual sites (not shown) reveals that the sites where no significant trend was identified in the observations have a particularly large inter-annual variability of PM concentrations. Model ensemble results identify significant trends at more sites compared with the observations, namely at 18 sites for PM_{10} and at 8 for $\text{PM}_{2.5}$. As can also be seen on the trend maps (Figure 2), the model ensemble and the observations do not always agree regarding the significance of trends at specific locations, even within the same country. For example in Spain,
 325 strong decreasing significant trends were observed at 4 out of 6 sites for PM_{10} and at 3 out of 4 sites for $\text{PM}_{2.5}$, whereas the model ensemble mostly estimates non-significant trends. This is in contrast to the German sites, for which the models simulate significant and quite appreciable PM_{10} and $\text{PM}_{2.5}$ trends for all sites (as a result of emission reductions in the whole country), but significant observed trends are found for only 3 out of 7 sites for PM_{10} and for 1 of 2 sites for $\text{PM}_{2.5}$. The reason for this seems to be that the trends were distorted by particular high annual mean PM concentrations in 2003, 2006 and 2010 at most
 330 of the German sites (not shown here).

Similar to Figure 5 for the model ensemble, Figure A7 presents PM_{10} and $\text{PM}_{2.5}$ mean trends calculated by the individual models, with only significant modelled trends shown. For any specific site, the trend slope values from the models are in general agreement (Figure A7), while there are discrepancies between the models with regards to the simulation of significant trends. The largest number of significant PM_{10} and $\text{PM}_{2.5}$ trends were simulated by EMEP (23 and 14, respectively) and the smallest
 335 number by MINNI (10 and 7) (see also Table 1).

The relative trends from the individual models are compared with each other and with observed relative trends in Figure A8 for the set of trend sites.

Averaged over all sites (see Table 1), the ensemble-modelled trends are -0.24 (ranging from -0.16 to -0.33 from the individual models) $\mu\text{g m}^{-3} \text{ year}^{-1}$ for PM_{10} and -0.21 (ranging from -0.19 to -0.26) $\mu\text{g m}^{-3} \text{ year}^{-1}$ for $\text{PM}_{2.5}$. The observed trends are
 340 stronger than the ensemble results, namely -0.35 and $-0.40 \mu\text{g m}^{-3} \text{ year}^{-1}$ respectively. Better agreement among the models is found for relative trends (ranging from -1.4 \%year^{-1} to -2.2 \%year^{-1} for PM_{10} and from -1.8 \%year^{-1} to -2.4 \%year^{-1} for $\text{PM}_{2.5}$) across those sites. The modelled relative trends compare quite well with the observed trends (-2.1 and 2.9 \%year^{-1} for PM_{10} and PM_{10} respectively) (Table 1).



5.3 PM seasonal trends

Figure 7 presents the maps of 2000-2010 seasonal mean trends of PM_{10} and $\text{PM}_{2.5}$ from the 6-model ensemble and the observations. For the winter season, the model ensemble estimates significant PM_{10} and $\text{PM}_{2.5}$ trends only in small areas, mostly in southern parts of Europe. The observational data do not show any significant trends for PM_{10} . For $\text{PM}_{2.5}$, the observations indicate quite strong significant trends at only three sites, i.e. in the north-east of Spain (also identified by the model ensemble), north Italy and south of Sweden. One probable reason for the limited number of sites with insignificant observed trends is negligible reductions and even increases in the emissions of primary PM from residential heating, most important in the winter period, which were not efficiently regulated.

For the summer period, both the model ensemble and observations estimate the strongest negative trends out of all seasons. Significant trends are simulated for most of the domain (except Northern Europe, south of Spain and most eastern parts of the domain). The number of sites with observed significant trends is also the strongest for summer, namely 12 out of 26 for PM_{10} and 10 out of 13 for $\text{PM}_{2.5}$. In the spring and autumn periods, both modelled and observed trend slope values and the fraction of sites with significant trends are between those of winter and summer.

It can be noted that Ispra in northern Italy (IT0004) is the only site where significant $\text{PM}_{2.5}$ trends were observed and calculated for all seasons, with the exception of the modelled winter trend. For PM_{10} , the quite strong significant mean trends at four Spanish sites (ES0007, ES0008, ES0013 and ES0014) appear to be due to strong summer trends, whereas the trends are insignificant in the other seasons. Among the German sites, significant observed PM_{10} trends are only identified at DE0001 and DE0007 and only for the spring period. The models agree with that, but also calculate significant trends for summer and autumn.

Figures 8 (a, b) present the annual series of the 6-model ensemble and observed seasonal mean trends of PM_{10} and $\text{PM}_{2.5}$ for the period 2000-2010, averaged over all trend sites. The values of absolute and relative trend slopes are summarized in Table 2.

Averaged over the trend-sites, the largest decrease in PM during the 2000-2010 period took place in the summer months for both PM_{10} , with the mean seasonal trend of $-0.32 \mu\text{g m}^{-3} \text{ year}^{-1}$ from the model ensemble and $-0.56 \mu\text{g m}^{-3} \text{ year}^{-1}$ from the observations, and for $\text{PM}_{2.5}$ (-0.26 and $-0.51 \mu\text{g m}^{-3} \text{ year}^{-1}$, respectively). The weakest trends were found for the winter season from the models and observations for PM_{10} (-0.13 and $-0.19 \mu\text{g m}^{-3} \text{ year}^{-1}$, respectively) and also for modelled $\text{PM}_{2.5}$ ($-0.10 \mu\text{g m}^{-3} \text{ year}^{-1}$), whereas the observed $\text{PM}_{2.5}$ trend has a minimum of $-0.27 \mu\text{g m}^{-3} \text{ year}^{-1}$ in the autumn season. The weakest winter trends are partly due to the larger amplitudes of the inter-annual changes in mean PM levels. In particular, the elevated winter levels of PM_{10} and $\text{PM}_{2.5}$ in 2006, and especially in 2010, contribute to reduce the mean seasonal trend.

Figure 9 presents the seasonal mean trends simulated by the individual models and the model ensemble, along with the observed trends. The graphs nicely visualize the seasonal variations of PM trend slopes discussed above. They also show quite a good correspondence between the trend seasonality from the individual models. Relative trends of PM show quite similar seasonal patterns, with the strongest trends in the summer and weaker ones in the cold seasons of 2000-2010 (Figure 9). For PM_{10} , observed relative trends are $-2.9 \% \text{ year}^{-1}$ in the winter period and $-3.7 \% \text{ year}^{-1}$ in the summer period; the respective



numbers from the model ensemble are -2.3 and $-2.5 \text{ \% year}^{-1}$. For $\text{PM}_{2.5}$, the observed and modelled summer trends are -3.7 and $-2.9 \text{ \% year}^{-1}$, whereas the weakest observed mean trend of $-2.0 \text{ \% year}^{-1}$ was in the autumn and the weakest modelled trend of $-1.4 \text{ \% year}^{-1}$ was estimated for the winter period. The individual models largely agree on the seasonal profiles of the relative trends, although some variability exists between the simulated trend slopes (similar to those for seasonal absolute trends).

5.4 Contribution of individual components to PM trends

PM_{10} and $\text{PM}_{2.5}$ is a complex mixture of different aerosol components originating from a variety of anthropogenic and natural emission sources and so PM trends are basically the sum of individual trends of its constituents. Thus, for a better understanding of the effects of emission reductions of different pollutants, it is imperative to look at the role of the individual aerosol components in the changes of PM concentrations.

A comprehensive study of the trends for individual aerosols is beyond the scope of this paper. Besides, there is practically no available observational data for individual PM components collocated with PM measurements during the period 2000-2010. In fact, Birkenes in the south of Norway is the only site for which observational data for both PM_{10} and $\text{PM}_{2.5}$, and for secondary inorganic aerosols (SIA) meet the required criteria for the trend study. Still, we think that for a better interpretation of PM trends discussed in this paper, it is relevant to have a brief insight into the trends of PM components. Here, we summarize the main results of modelled and observed trends of some PM components for 2000-2010. For more a detailed analysis of inorganic gases and aerosols, the reader is referred to Ciarelli et al. (2019).

Figure A9 shows the maps of model ensemble simulated and observed annual mean 2000-2010 trends for SO_4^{2-} , NO_3^- and NH_4^+ aerosols. Note that due to the lack of consistent observational data sets (as pointed out above), the set of sites for SIA are not the same and also different from those used in PM trend analysis. The number of sites used here is 39, 14 and 13 for SO_4^{2-} , NO_3^- and NH_4^+ .

The absolute trends are all decreasing, though the rates are not directly comparable (since they are expressed as $\mu\text{g m}^{-3} (\text{S}) \text{ year}^{-1}$ and $\mu\text{g m}^{-3} (\text{N}) \text{ year}^{-1}$). The maps of relative trend slopes show the strongest trends all over Europe for SO_4^{2-} (between -2 and -4 \% year^{-1} over most of the domain, exceeding -5 \% year^{-1} in Spain), closely followed by NH_4^+ . For NO_3^- , the models only estimated significant downward trends in Central European countries and Italy. The modelled trends for SIA are decreasing over the entire domain, whereas the observations indicate significant increasing trends of SO_4^{2-} and NO_3^- at the Polish site Sniezka (close to the Czech border). In addition, rather strong, though non-significant, positive trends of NO_3^- and NH_4^+ were observed at two Dutch sites, and somewhat weaker positive trends at a few other sites. No observational datasets long enough (or obtained with consistent analytical methods) for trend studies of carbonaceous aerosols were available at EMEP sites. Shorter series for total carbon, available for three-four sites, show a 4-5% decreasing trend between 2003/2004 and 2010. In summary, the results presented here, and the analysis by Ciarelli et al. (2019), indicate that the models estimate a somewhat larger than observed decrease of SO_4^{2-} in Central (also missing some positive trends) and Northern Europe and a smaller decrease in Spain. The models appear to overestimate the observed negative trends for NO_3^- and also for NH_4^+ , though



to a smaller degree (one should keep in mind that for NO_3^- and NH_4^+ there is limited number of measurement sites covering a limited geographic area).

The relative contributions of SO_4^{2-} , NH_4^+ , NO_3^- , total primary particulate matter (TPPM₁₀) and anthropogenic SOA (ASOA) to PM₁₀ trends in the period 2000-2010 estimated by the model ensemble are presented in Figure 10. The maps reveal considerable variability of the role of the individual aerosols in PM₁₀ trends across European countries. The decrease in SO_4^{2-} concentrations (Figure 10a) played the dominating role in many parts (particularly in Spain, the Baltic countries and Russia), but not in Germany, France, the UK or Norway. Germany, Denmark and Northern Italy (the Po Valley) are the regions with relatively large contributions of NO_3^- to PM₁₀ trends compared with the rest of the simulation domain (Figure 10c). The reduction of NH_4^+ levels, which includes both ammonium sulphate and ammonium nitrate, appears to be a very important contributor to the PM₁₀ decreasing trends, with the largest effects calculated for Poland, Denmark, and the Po Valley (Figure 10b). The reduction of primary PM emissions was according to the model ensemble simulations the dominating factor for PM₁₀ trends in France, Norway, Portugal, Greece and parts of the UK and Russia (Figure 10d). Finally, ASOA is also estimated to have quite a notable contribution of 3-7% to PM₁₀ downward trends (though ASOA modelling is still associated with rather large uncertainties). The model results imply that the chemical composition of European PM₁₀ has changed somewhat during the 2000-2010 period, with NO_3^- (and probably ASOA) becoming an increasingly important constituent compared with the other anthropogenic aerosols, i.e. SO_4^{2-} , NH_4^+ and primary emitted PM (elemental and primary organic carbon, dust and metals).

The relative contributions of SO_4^{2-} , NH_4^+ , NO_3^- , and ASOA to PM₁₀ trends in the period 2000-2010, as calculated by the individual models can be found in Appendix (Figure A11). The models, with the exception of LOTO and POLR, agree that over most parts of Europe (though not in Germany), decreases in SO_4^{2-} and NH_4^+ concentrations were the main cause of PM₁₀ downward trends, with somewhat smaller contribution from decreasing NO_3^- levels. This is consistent with the emission trends shown in Figure A1. The largest emission reductions achieved for SO_x explains the relatively strong SO_4^{2-} and NH_4^+ (in the form of ammonium sulphate) trends. The reductions of NO_x and NH_3 emissions from 2000 to 2010 were smaller compared with SO_4^{2-} . Thus, as the formation of ammonium sulphate was decreasing in the 2000s, more and more NH_3 was becoming available for the formation of ammonium nitrate NH_4NO_3 . Notably in Germany, as well as in the Benelux countries and the Po Valley, NO_3^- is estimated by the models to have the largest contribution to the PM₁₀ trends. Furthermore, the estimates by LOTO point to primary anthropogenic PM₁₀ as the main component driving PM₁₀ levels down in a large part of the simulation domain. CHIM, MINNI and to some extent EMEP agree with the LOTO estimates for Northern Europe and the area covering Benelux, northern parts of Germany and France, and the south of the UK. In contrast to the other models, POLR estimated that NH_4^+ contributed the most to the PM₁₀ trends, whereas the contribution of SO_4^{2-} and NO_3^- were rather moderate according to POLR. The modelled contributions of ASOA to PM₁₀ trends is below 5% according to CHIM, MATCH and MINNI, whereas EMEP simulates contributions of 5-10% and POLR 5-30%. This variability can be explained by the different ways of handling SOA chemistry in the models. Furthermore, somewhat weaker PM trends from LOTO could probably be explained by not including SOA chemistry in these simulations. Similar results are seen with respect to the relative contributions of the individual aerosols to modelled PM_{2.5} trends between 2000 and 2010 (Figure A12).



As far as natural aerosols are concerned, emissions are largely driven by meteorological conditions (e.g. by the surface wind in the case of sea salt and windblown dust, while the air temperature controls emissions of biogenic VOCs - precursors of biogenic secondary organic aerosol, BSOA). In addition, the generation of mineral dust is dependent on the availability of erodible (snow and vegetation free) soil and its moisture (which in turn depends on precipitation frequency and amount),
450 whereas the temperature and salinity of sea water affect sea spray formation, though those conditions are less variable. Of course, similar to anthropogenic aerosol, the transport and removal of the natural particles are determined by atmospheric dynamics and precipitation. In short, year-to-year changes in the concentrations of natural aerosols are driven primarily by inter-annual meteorological variability. Among natural aerosols, only BSOA have some dependency of anthropogenic emissions, as they can be formed from biogenic VOCs condensing on primary organic aerosols from anthropogenic sources. Thus, BSOA
455 production is somewhat affected by the trend in PM emissions.

Not all natural particles were calculated in a consistent way by all of the models. The missing components are: BVOC from LOTO and MATCH, sea salt from POLR; and only EMEP and LOTO simulated trends of windblown dust in the modelling domain, whereas the other models only included mineral dust from boundary conditions. Figures 10 (f, g, h) present the computed contributions of natural aerosols estimated by the models, i.e. biogenic SOA, sea salt and mineral dust, to PM₁₀
460 trends, where the negative contributions (blue colours) mean increasing trends in the natural aerosols.

The model ensemble simulated decreasing BSOA trends that contribute 1-3 % of PM₁₀ decreasing trends over almost all land area (Figure 10f), with the largest contribution (5-10%) in Fennoscandia and north-western Russia. The contribution of sea salt trends (derived as 3.26*sea salt Na) to PM₁₀ trends is, on average, 2-5 % over land and exceeds 10 % in areas influenced more by the sea and less polluted regions (Figure 10g). Comparison of the modelled sea salt trend with rather sparse
465 observations can be found in Figure A10 (a).

Furthermore, from the EMEP and LOTO results, we see contributions of 1-3% from mineral dust to decreasing PM₁₀ trends over most of Europe (in excess of 10% in Spain, Italy), but also some negative contributions due to increasing dust trends in Greece, Portugal and south-eastern Europe and Russia (Figure 10h). All in all, the inter-annual variability and increasing modelled trends for natural aerosols for some regions do not appear to have reversed the decreasing PM₁₀ trends in the 2000-
470 2010 period (with some exceptions for windblown dust).

Model analysis of the seasonal trend of the individual PM₁₀ and PM_{2.5} components shows the strongest trends of SIA (SO₄⁻², NH₄⁺ and NO₃⁻) in summer and also in spring for NO₃⁻, while the weakest trends of all SIA are calculated for winter. On the contrary, the strongest trends for primary PM are simulated for winter and the weakest for summer.

6 PM trends in the period 1990 – 2010

475 As no regular measurements of PM were conducted prior to 2000, this paper mainly focus on the period 2000-2010. As far as the years prior to 2000 are concerned, we have to rely solely on model simulations to assess the effect of emission reductions on European levels of particulate pollution in the 1990s. Given that, any deep analysis of that decade is beyond the scope of the paper, but still we think it is relevant to present a multi-model assessment of PM trends during the whole 1990-2010 period,



studied within the EDT framework. It should be kept in mind while looking at those results, that the emission data, in particular
 480 for PM₁₀, are much less reliable before 2000.

Figure A13 shows annual mean trends for the period 1990-2010 for PM₁₀ and PM_{2.5}, absolute and relative to 1990, produced by the ensemble of five models (all the above except POLR). Over the whole European domain, the models simulate significant decreasing PM trends. The strongest trends ($0.75\text{--}1.0\ \mu\text{g m}^{-3}\text{ year}^{-1}$, or $2.5\text{--}3\ \%\text{ year}^{-1}$) were simulated for Central Europe (extending eastward over Ukraine and European Russia for PM_{2.5}). The weakest trends of less than $0.3\ \mu\text{g m}^{-3}\text{ year}^{-1}$
 485 ($1.5\text{--}2\ \%\text{ year}^{-1}$) are seen in Northern Europe and Russia and in Southern Europe. The rest of the domain experienced intermediate trends of $0.3\text{--}0.75\ \mu\text{g m}^{-3}\text{ year}^{-1}$ ($1.5\text{--}2.5\ \%\text{ year}^{-1}$ relative to the year 1990). Notably, the weakest decreasing trends (below $1.5\ \%\text{ year}^{-1}$) are modelled for PM₁₀ in the southernmost parts of Mediterranean countries, which are heavily influenced by Saharan dust and so PM trends due to the reductions of anthropogenic emissions are distorted. The mean annual trends during the period of 1990-2010 are stronger compared with those for the 2000-2010 period (Figure 2). This is a consequence
 490 of larger emission reductions in the 1990s compared with the 2000s. Thus, the EDT model ensemble simulated that annual mean PM₁₀ and PM_{2.5} concentrations decreased by between 5 and $15\ \mu\text{g m}^{-3}$ across most of Europe (by $2\text{--}5\ \mu\text{g m}^{-3}$ in the Northern Europe) from 1990 to 2010.

6.1 PM trends in European countries in 1990-2000-2010 periods

The graphs in Figure A14 provide more details regarding PM₁₀ trends in individual European countries and compare the
 495 trends in the 1990s and 2000s.

Figure A14a shows the trends of PM₁₀ between 1990 and 2010 simulated by the five models for the individual countries and sea areas. The strongest annual mean trends (leftmost countries in the graph) were simulated for Central European (Germany, Hungary, Czech Republic) and the Benelux countries, which were the regions with among the highest PM levels. The weakest downward trends are modelled for relatively cleaner North European (Iceland, Norway, Finland, Sweden) and Baltic countries,
 500 but also in Mediterranean countries influenced by shipping emissions and African dust intrusions (rightmost countries in the graph). The models are in general agreement regarding the ranking of PM₁₀ national trends, and the spread between PM national trends calculated with the individual models is rather moderate. The variation of PM_{2.5} trends across Europe is quite similar (therefore not shown here), with the only difference that the trends in the Benelux countries were the strongest.

Figure A14b shows for the individual countries and regions, the PM₁₀ annual trends calculated by the model ensemble for
 505 the 1990-2000 and the 2000-2010 periods separately. For most of the countries, the largest reductions of PM₁₀ levels took place in the 1990s compared with the 2000s. This is especially pronounced in Central Europe, where the 1990-2000 trends were around $1\ \mu\text{g m}^{-3}\text{ year}^{-1}$ compared with around $0.3\ \mu\text{g m}^{-3}\text{ year}^{-1}$ in the 2000-2010 period. The exceptions are North-European countries, and also relatively small emitters of pollution, such as Malta, Liechtenstein, Cyprus, where PM₁₀ trends were similar during both decades.

510 The PM₁₀ relative trends (i.e. with respect to the starting years of 1990 and 2000) in the 1990-2000 period are also considerably stronger than those in the 2000-2010 period (not shown, or in Supplement). The model results indicate a large variability in 1990-2000 trends between the countries (from $-1.1\ \%\text{ year}^{-1}$ in Central Europe to $-(0.0\text{--}0.2)\ \%\text{ year}^{-1}$ in Northern Eu-



rope, Cyprus, Malta), whereas the 2000-2010 trends are more homogeneous across the countries, ranging between 0 and -3 % year⁻¹.

515 7 Discussion

7.1 Discussion of main results

The ensemble of six EDT models simulated that, from 2000 to 2010, the annual mean PM₁₀ and PM_{2.5} concentrations decreased by between 10 and 20% over most of Europe, and respectively by up to 25% and 30% in Germany, the Netherlands, Belgium, parts of the UK, Portugal, north/centre of Italy and large parts of Scandinavia. Notably, despite lower PM_{2.5} concentrations, the PM_{2.5} absolute downward trends appear only slightly smaller than those for PM₁₀, indicating a trend-masking role of coarse PM of natural origin. On average, we found a fair agreement between modelled and observed concentration reductions at 26 (for PM₁₀) and 13 (for PM_{2.5}) measurement sites. In the course of those 11 years, PM₁₀ and PM_{2.5} concentrations at the studied sites decreased respectively by 17 and 20% according to the model ensemble and by 21 and 29% as derived from observational data. Moreover, we found a larger spatial variability of PM trends registered by observations compared with those estimated by the model, with observed decreasing trends ranging between approximately 5% (at British site GB0036) and 50% (at Swedish site SE0012). We also see some discrepancies in the geography of trends from the observations and EDT model, with the largest observed decreases (above 30%) at the sites in Sweden, Finland and Spain (also the Po Valley for PM_{2.5}), whereas the models simulate the strongest trends for German sites (mostly above 20%) and do not identify significant trends for Spanish sites (though 10–20% decreases in PM₁₀ and PM_{2.5} is simulated).

Modelled PM concentrations are to a large degree determined by the emission data used and modelled PM trends reflect the trends in national emissions. For instance, relatively strong simulated PM trends in Germany, the Benelux, the UK and Portugal are due to considerable reductions of all gaseous precursors and primary PM in those countries (Figure A2). Poland is among the countries with the greatest reduction of SO_x and considerable reductions in NO_x emissions from 2000 to 2010, but the increase in NH₃ emissions contributed to additional SIA formation during those years. Besides, the emissions of primary PM_{2.5} went up in the same period. Thus, the resulting modelled downward trends are relatively weaker (and insignificant in parts of the country). In Northern Europe, the appreciable decrease of PM concentrations is not only due to reductions in NO_x and primary PM_{2.5} emissions in those countries, but is also due to decreased long-range transport from Central Europe and the UK (somewhat lessened by the increased NO_x emissions from international shipping in the North and Baltic seas). For Spain, the models simulated a substantial decrease in PM concentrations (though the PM trends were characterised as insignificant), mostly resulting from emission reductions of gaseous precursors, while the reductions in emissions of primary PM (especially coarse PM) were relatively smaller.

Furthermore, the analysis showed a considerable variability in the observed trends within the same country, which the models could not fully reproduce. This can be due to local emissions, unaccounted for, or misrepresented spatially in the model input. In some countries, the differences in trends could also be related to a complex topography leading to localised pollution transport dynamics (e.g. Switzerland and Austria), unresolved by meteorological drivers.



As PM is a complex pollutant, consisting of different aerosol species, the concentrations and trends of PM are the result of an intricate interplay of the effects of their direct emissions and gaseous precursors from a variety of anthropogenic and natural sources. As discussed in Section 4, the emissions of SO_x went down by 37% from 2000 to 2010, resulting in the decrease of ammonium sulphate concentrations and thus more ammonia available for reactions with nitric acid. The reduction of NO_x emissions in the same period (17%) was smaller than that of SO_2 . Given rather moderate reductions of NH_3 emissions (only 6% on average), the concentrations of ammonium nitrate decreased less compared with ammonium sulphate. The model ensemble calculated the decrease for SO_4^{2-} to be in a range of 25-45% (45-55% in Spain and Portugal) and for NH_4^+ in a range of 15-40% over Europe from 2000 to 2010 (Figure A9, a-f). The modelled decrease of NO_3^- concentrations is mostly under 30% and the trends are insignificant in most countries. For more detailed discussion on SIA trends, we refer the reader to the analysis published in (Ciarelli et al., 2019). In that publication, relatively moderate trends in SO_4^{2-} compared with the emission reductions of SO_2 was explained by an increase in the availability of oxidant species and more efficient pH-dependent cloud chemistry resulting from those emission reductions. (Ciarelli et al., 2019) also discusses a shift in the thermodynamic equilibrium between $\text{HNO}_3 + \text{NH}_3$ vs. NH_4NO_3 , favouring aerosol formation. Furthermore, the reduction of anthropogenic VOC emissions, including aromatic hydrocarbons - precursors of SOA, by 33%, on average, led to a decrease in ASOA concentrations by 15-30% from 2000-2010 (Figure A9, g, h). Finally, the emissions of both $\text{PM}_{2.5}$ and coarse PM reduced, on average, over the modelled domain by 10%, thus making primary PM an important driver of PM_{10} and $\text{PM}_{2.5}$ decreases in some European regions (not shown here).

Due to the lack of long-term observational data of PM_{10} and $\text{PM}_{2.5}$ supplemented with chemical analyses, the model results regarding the role of the individual components in PM_{10} and $\text{PM}_{2.5}$ trends during 2000-2010 cannot be thoroughly validated. We can only make a crude estimate, using observations of SIA and OC, which are not necessarily collocated, available at a limited number of sites. The observed average trends were the strongest for organic aerosols (-3.8 \%year^{-1} at 4 sites), followed by NH_4^+ (-2.9 \%year^{-1} at 13 sites), SO_4^{2-} (-2.6 \%year^{-1} at 39 sites), and finally the weakest trends were for NO_3^- (-0.5 \%year^{-1} at 14 sites).

7.2 Uncertainties in emissions

As shown in the previous section, the modelled trends in PM and its components quite closely reflect emission reductions, though inter-annual variability of meteorological conditions also plays an important role in PM pollution levels (see 7.3). This means that good quality emission data is essential for accurate model simulations of the trends.

Emission estimates are associated with uncertainties due to missing or incomplete information, or limited understanding with respect to activity data, emission factors, source locations etc. (Klimont et al., 2017).

No publication with a detailed and quantitative uncertainty estimate of the GAINS dataset used here (ECLIPSE_V5) is available, but (Amann et al., 2011) and (Schöpp et al., 2005) described the treatment of uncertainties in the context of the GAINS model. For example, for 1990, (Schöpp et al., 2005) estimated that the national total emissions used in the RAINS integrated assessment model had an uncertainty of $\pm 6\text{--}23\%$ for SO_2 , $\pm 8\text{--}26\%$ for NO_x and $\pm 9\text{--}23\%$ for SO_2 . However since that assessment, steps have been taken to reduce the uncertainty in the emission data sets (Klimont et al., 2017). The



580 European Environment Agency indicated somewhat larger uncertainties in typically top-down emission estimates in the EU LRTAP inventory, namely $\pm 10\%$ for SO_2 , $\pm 20\%$ for NO_x and $\pm 30\%$ for SO_2 (EEA, 2008). Clearly, underestimation of emissions would lead to underestimation of the absolute trends of PM.

Furthermore, EEA (2008) suggested that the emission trends are likely to be more accurate than the individual absolute annual values, although the use of gap-filling when countries have not reported emissions for one of more years can potentially
585 lead to artificial trends. Regarding primary PM emissions, ECLIPSE_V5 was the first assessment of PM_{10} and $\text{PM}_{2.5}$ emissions, performed using a consistent bottom-up approach across all sources and regions and, therefore, only limited comparison to other works was possible (Klimont et al., 2017).

One of the biggest sources of emissions-related uncertainty is likely to be residential wood-burning emissions of PM and VOCs (forming ASOA) (Simpson et al.). Emissions of primary organic matter (POM) from residential wood burning have
590 been known to be problematic for many years (Denier van der Gon et al., 2015; Simpson and Denier van der Gon, 2015), with different countries accounting for, or omitting, semi-volatile compounds in different and often unknown ways. Given that wood burning for heating houses accounts for a significant percentage of European PM emissions, the lack of consistent treatment between countries has obvious implications for the reliability of any trend estimates. There is an increasing recognition that emissions of some potentially important SOA precursors, namely semi-volatile and intermediate-volatility organic compounds
595 (SVOC, IVOC) from traffic sources, are also missing from national inventories and these can have significant impacts on ambient organic matter (OM) (Ots et al., 2016). Emissions of SVOCs and IVOCs are very dependent on e.g. the fuel and type of catalyst used in cars (Jathar et al., 2014; Platt et al., 2017), with older vehicles likely emitting substantially more than new ones, again complicating any analysis of trends. Even for the same country, condensable organics might be included or excluded differently for different sectors. Inclusion or exclusion, or the extent of inclusion of condensables, has also changed
600 over the years, which directly affects the accuracy of trend analyses (Aas et al., 2021). Finally, with respect to anthropogenic sources, assumed invariant spatial distribution of emissions (except from industrial sectors) may cause inaccuracy in modelled trends in some areas.

As far as natural emissions are concerned, biogenic VOC (BVOC) emissions estimates have also many uncertainties, both for isoprene and monoterpenes (e.g. Simpson et al., 1999; Langner et al., 2012; Messina et al., 2016). The models in this study
605 calculate BSOA formed from the oxidation of isoprene and terpenes (CHIMERE also includes sesquiterpenes), but additionally BSOA can also be formed from the oxidation of stress-induced emissions of other VOCs that are not included in the emissions; this process is likely to be quite frequent, but can only be accounted for in speculative terms with current knowledge (Bergström et al., 2014). Beside uncertainties in emission estimates, the emission data used in the model runs omit some sources of PM. Among the omitted sources of OM are primary biological material, which can contribute e.g. 20-30% of PM_{10} in Nordic areas
610 in summer-early autumn (Yttri et al., 2011) (though it is likely to be much less as an annual average (Winiwarter et al., 2009)). Marine sources of OM also contribute to observed ambient OM (e.g. Spracklen et al., 2008), but the models used here have not accounted for those (some models, such as EMEP, have assumed background levels of OM which account for such diverse sources, but only in a crude way and with the same levels assumed for all years).



7.3 Effect of inter-annual meteorological variability

As pointed out in Section 2.3, the probability of trend detection using the Mann-Kendall method decreases for shorter data-series, large natural variability and relatively weak trends. The bottom-line is that the weaker the trend is relative to the inter-annual meteorological variability, the longer the time series that is needed in order to identify a significant trend. As estimated in https://wiki.met.no/_media/emep/emep-experts/mannkendall_note.pdf, for an 11-year time series and -2 to -3% year⁻¹ trends, the fraction of significant trends identified by MK test will be between 92 and 100% for an inter-annual meteorological variability of 5%, dropping down to between 37 and 71% for a 10% variability and even further down to between 19 and 39% for a 15% variability. For weaker trends of -1% year⁻¹, the corresponding probabilities are only 36, 13 and 9% for an inter-annual meteorological variability of 5, 10, and 15%.

The model simulations performed in this work indicate that the relative inter-annual variability of PM concentrations due to meteorological variability is by far and large below 15% relative to the 11-year mean. It varies mostly between 5 and 10% over Central/Eastern Europe with somewhat larger variability over Northern Europe and Iberian Peninsula during 2000-2010 (not shown here). This can explain the large number of sites (and areas) where the models do not estimate significant trends in the 2000-2010 period, given that average PM trends are between 1 and 3% year⁻¹. Still, the observations indicate even more sites with non-significant PM trends with respect to the models.

In addition, we have looked at the relative effects of emission changes and inter-annual meteorological variability on PM trends by calculating the so-called normalised relative trends (NRT) introduced in Solberg et al. (2009) and also applied in Colette et al. (2011). For this purpose, we used additional model results obtained from model runs with fixed 2010 emissions for the meteorological conditions 1990 to 2010 (i.e. Tier 3B as described in Colette et al. (2017a)). The effect of the emissions on PM trends was assumed to be represented by the difference in PM concentrations obtained for corresponding years in the trend runs (Tier3A) and the runs with constant emissions (Tier3B); and the inter-annual variability due to meteorological conditions was quantified by standard deviation of annual PM concentrations in the runs with constant emissions. That is to say, we calculated the ratio of the difference of Sen's slopes ($PM_{Tier3A} - PM_{Tier3B}$) to $STD(PM_{Tier3B})$. The model ensemble NRT for PM_{10} and $PM_{2.5}$ are presented in Figure 11, where absolute NRT values greater than one indicate a larger importance of emission changes with respect to the inter-annual meteorological variability.

Figure 11 shows that the effect of emission reduction on decreasing PM trends appears to be downsized by inter-annual meteorological variability in large part of Europe in the 2000-2010 period. It should be noted that the individual EDT models have different sensitivity to meteorological variability (besides MATCH and LOTO used different meteorological drivers), which may mask the effects of emission changes. The emission reductions play a larger role in $PM_{2.5}$ trends, as PM_{10} concentrations (particularly the coarse fraction of natural origin) are more affected by variability in meteorological conditions. Evidently, the most pronounced effects of emission reductions are associated with the regions with greater emission reductions, e.g. Portugal, Benelux, some parts of South-Eastern European and the Balkan countries. These results are consistent with the main conclusions from the study of PM trends in the period 1998-2007 by Colette et al. (2011). Colette et al. (2017b) arrived to somewhat different conclusions based on a different approach, namely the decomposition of the differences in EDT



modelled PM concentrations in 2000 and 2010 to discriminate the role of emissions, meteorology and boundary conditions. Their analysis suggested a relatively larger on average role of emissions compared with the meteorology, though the estimated
 650 uncertainties were non-negligible. Due to different premises used by Colette et al. (2017b) and this paper, discrepancies in the outcomes are to be anticipated. That is, here we compared 11-year PM trends with year-to-year PM variability due to meteorological conditions, whereas Colette et al. (2017b) looked at the difference between 2010 and 2000.

To summarise, given rather moderate reductions (and even some increases) in the emissions of some PM precursors and primary PM between 2000 and 2010, we estimate that the effect of emission decreases on 2000-2010 PM trends is roughly of
 655 the same order of magnitude as the effect of inter-annual meteorological variability. Separating the effects of emission changes and meteorological variability on PM trends, we get additional insights regarding their relative roles. PM trend slopes due to emission trends (Figure 11) appear to be quite similar to the total trends wherever the latter are more significant (Figure 2). The remarkable difference between them is that the trends due to emissions are significant for nearly the entire domain. Model simulated PM trends due to solely inter-annual meteorological variability (not shown) are by far and large very small (\pm
 660 $0.05 \mu\text{g m}^{-3} \text{yr}^{-1}$) and non-significant everywhere. Thus, our results suggest that the main impact of variable meteorological conditions is to reduce the significance level of PM trends due to emission reductions, while the effects on PM trend slopes are much smaller. For comparison, since the emission reduction during the 1990s were overall larger than in the 2000s, the effect of emission reductions on the decreasing PM trends is estimated to dominate meteorological variability in most of Central, Eastern and South-Eastern Europe (Figure 11).

665 8 Summary and outlook

The Eurodelta-Trends multi-model experiment, aimed to assess the efficiency of emission mitigation measures in improving air quality in Europe, was designed to answer a series of questions regarding European pollution trends in the period of 1990-2010. Among these questions are: Were there significant trends detected by observations? Do the models manage to reproduce observed trends? How close is the agreement between the models and how large are the deviations from observations? In this
 670 paper, we address these issues with respect to PM pollution.

An in-depth trend analysis has been performed for PM_{10} and $\text{PM}_{2.5}$ for the period of 2000-2010 (limited by the availability of observations), based on results from six CTMs and observational data from the EMEP monitoring network. Given harmonization of set up and main input data (with a few exceptions), the differences in model results should mainly result from differences in the process formulations within the models themselves, and the spread in the models simulated trends could be
 675 regarded as an indicator for modelling uncertainty.

The results of the analysis strongly indicate overall decreasing trends of annual mean PM_{10} and $\text{PM}_{2.5}$ concentrations between 2000 and 2010, although the trends are not characterized as significant everywhere. The model ensemble simulated mean negative trends that vary from below $0.1 \mu\text{g m}^{-3} \text{yr}^{-1}$ in northern Europe to $0.1\text{--}0.4 \mu\text{g m}^{-3} \text{yr}^{-1}$ in the eastern parts, and to $0.4\text{--}0.7 \mu\text{g m}^{-3} \text{yr}^{-1}$ in central Europe and most of the UK, with $\text{PM}_{2.5}$ negative trends being slightly weaker than
 680 those for PM_{10} . That would mean that annual mean PM concentrations decreased by between 2 and $6 \mu\text{g m}^{-3} \text{m}^{-3}$ over



Europe during the 2000-2010 period. In relative terms, the decrease of annual mean PM_{10} and $\text{PM}_{2.5}$ was between 10 and 20% over most of Europe (up to 25-30% in Germany, the Netherlands, Belgium, parts of the UK, Portugal, north/center of Italy and large parts of Scandinavia) from 2000 to 2010. We find that the modelled PM trends are fairly consistent with emission reductions in the ECLIPSE_V5 data set used here. Among possible reasons for deviations between the models and observations
 685 are emission uncertainties, impacts of inter-annual variability in meteorological conditions (on pollutant transport and removal, secondary aerosol formation, natural PM emissions etc.), model uncertainties associated with aerosol formation and removal processes (e.g. SOA formation, cloud pH dependency of SO_4 formation, thermodynamics, SO_2 and NH_3 co-deposition etc.). Furthermore, we find a fairly good general agreement in PM trends estimated by the individual models, with the inter-model variability below 30-40% over much of Europe (up to 50-60% in northern and eastern parts of EDT domain). Somewhat greater
 690 variability in the modelled PM_{10} trends reflects larger uncertainties in modelling of the coarse fraction of PM, which is mostly due to natural origin.

Averaged over measurement sites (26 for PM_{10} and 13 for $\text{PM}_{2.5}$), the mean ensemble simulated trends are $-0.24 \mu\text{g m}^{-3} \text{ year}^{-1}$ for PM_{10} and $-0.21 \mu\text{g m}^{-3} \text{ year}^{-1}$ for $\text{PM}_{2.5}$, which are somewhat weaker than the observed trends of -0.35 and $-0.40 \mu\text{g m}^{-3} \text{ year}^{-1}$, respectively. This is partly related to models' underestimation of PM concentrations. The correspondence
 695 between model results and observations appears better in terms of relative trends for the same period, which are -1.7 and -2.0% year^{-1} from the model ensemble and -2.1 and -2.9% year^{-1} from the observations for PM_{10} and $\text{PM}_{2.5}$ respectively. We see somewhat larger spatial variability of observed PM trends with respect to the modelled trends across Europe and within individual countries, which could partly be explained by the uncertainties associated with national sectoral emissions and their spatial distribution. In addition, the regional models have difficulties to accurately resolve pollution at some of the sites located
 700 in the regions with complex topography. The observations identify significant trends for PM_{10} at 56% of the sites and for $\text{PM}_{2.5}$ at 36% of the sites, which is somewhat less than those identified by the models.

The strongest decreasing trends and the largest number of sites (and larger areas) with significant trends were observed and modelled for summer concentrations of PM_{10} and $\text{PM}_{2.5}$. On the other hand for the winter season, the model ensemble identifies significant PM trends for very limited areas, mostly in southern parts of Europe, whilst the observed trends are not
 705 significant at any of the sites for PM_{10} and only at 3 out of 14 sites for $\text{PM}_{2.5}$. One important reason for that is the very modest reductions and even increases in the emissions of primary PM from residential heating in winter.

The analysis reveals a considerable variability of the role of the individual aerosols in PM_{10} trends across European countries. The multi-model simulations, supported by available observations, point to decreases in SO_4^{2-} concentrations playing an overall dominant role, although with some exceptions. Namely, we see relatively large contributions of the trends of NH_4^+
 710 and NO_3^- to PM_{10} decreasing trends in Germany, Denmark, Poland and the Po Valley, while the reductions of primary PM emissions appears to be a dominant factor in bringing down PM_{10} in France, Norway, Portugal, Greece and parts of the UK and Russia.

The analysis also suggests that year-to-year variability in meteorological conditions masks decreasing PM trends due to emission reductions, leading to non-significant trends in many areas and at many monitoring sites between 2000 and 2010.
 715 Still, the role of emission reduction measures is pronounced in the regions with greater reductions, where significant trends



of PM_{10} and $\text{PM}_{2.5}$ are both modelled and observed. The EDT model results show that the mean annual trends during the period of 1990–2010 were stronger compared with those in the 2000–2010 period, which is a consequence of larger emission reductions in the 1990s compared with those in the 2000s. The EDT model ensemble estimates that annual mean PM_{10} and $\text{PM}_{2.5}$ concentrations decreased by between 5 and 15 $\mu\text{g m}^{-3}$ across most of Europe (by 2–5 $\mu\text{g m}^{-3}$ in the Northern Europe) from 1990 to 2021.

Data availability. Technical details of the EURODELTA project simulations that permit the replication of the experiment are available on the wiki of the EMEP Task Force on Measurement and Modelling (<https://wiki.met.no/emep/emep-experts/tfmmtrendeurodelta>, last access: 22 November 2021), which also includes ESGF links to corresponding input forcing data. The EURODELTA Trends model results are made available for public use on the AeroCom server (information to gain access to the AeroCom server are available at <https://wiki.met.no/aerocom/user-server>, last access: 22 November 2021). Model input and output data are permanently stored under the /metno/aerocom-users-database/EURODELTA folder on the AeroCom Server. See Colette et al. (2017) for full terms and conditions for the use of these data.

The original data used for calculating aggregated concentrations are all available from the database infrastructure EBAS (<https://ebas.nilu.no>)



9 Tables and Figures

Table 1. Observed and modelled (ensemble mean and individual models), PM₁₀ and PM_{2.5} annual mean trends for the period 2000-2010, averaged over all trend-sites. The standard deviation is included in parentheses. Units are $\mu\text{g m}^{-3} \text{ year}^{-1}$ and $\% \text{ year}^{-1}$ for absolute (Abs) and relative (Rel) trends, respectively. The number of sites with significant trends identified by observations and models (Nsign) is also provided.

Parameter	Trends	Obs	ENSmean	CHIM	EMEP	LOTO	MATCH	MINNI	POLR
PM ₁₀ 26 sites	Abs	-0.35(0.23)	-0.24(0.09)	-0.22(0.09)	-0.33(0.11)	-0.23(0.11)	-0.27(0.08)	-0.24(0.10)	-0.16(0.16)
	Rel	-2.1(1.19)	-1.7(0.4)	-1.6(0.36)	-2.2(0.36)	-1.6(0.60)	-2.1(0.43)	-1.6(0.41)	-1.4(1.27)
	Nsign	14		14	23	16	20	10	14
PM _{2.5} 14 sites	Abs	-0.40(0.38)	-0.21(0.10)	-0.21(0.1)	-0.26(0.12)	-0.19(0.11)	-0.21(0.08)	-0.21(0.1)	-0.21(0.14)
	Rel	-2.9(1.48)	-1.6(0.33)	-1.8(0.35)	-2.4(0.43)	-2.0(0.53)	-1.9(0.40)	-1.8(0.44)	-2.1(0.77)
	Nsign	5		9	12	8	11	7	8

Table 2. Observed (Obs) and modelled (6-model ensemble; ENS) mean seasonal trends for 2000-2010 at all trend-sites. The numbers of sites with significant trends are in parentheses

Parameter		winter	spring	summer	autumn
PM ₁₀	Obs ($\mu\text{g m}^{-3} \text{ year}^{-1}$)	-0.19 (0)	-0.33 (7)	-0.56 (17)	-0.25 (7)
	ENS ($\mu\text{g m}^{-3} \text{ year}^{-1}$)	-0.13 (3)	-0.28 (10)	-0.32 (17)	-0.26 (7)
PM _{2.5}	Obs ($\mu\text{g m}^{-3} \text{ year}^{-1}$)	-0.38 (3)	-0.42 (4)	-0.51 (10)	-0.27 (2)
	ENS ($\mu\text{g m}^{-3} \text{ year}^{-1}$)	-0.10 (1)	-0.23 (3)	-0.26 (8)	-0.24 (7)
PM ₁₀	Obs ($\% \text{ year}^{-1}$)	-1.4	-1.8	-2.9	-1.6
	ENS ($\% \text{ year}^{-1}$)	-1.0	-1.8	-2.4	-1.8
PM _{2.5}	Obs ($\% \text{ year}^{-1}$)	-2.8	-2.7	-3.8	-2.0
	ENS ($\% \text{ year}^{-1}$)	-0.9	-1.8	-2.5	-2.1



	CHIM	EMEP	LOTO	MATCH	MINNI	POLR	mean
2000	-2	2	-6	-11	-4	-24	-8
2001	-4	-8	-4	-9	-8	-30	-11
2002	-7	-14	-13	-16	-14	-35	-17
2003	-8	-13	-16	-12	-12	-36	-16
2004	-7	-14	-10	-14	-9	-33	-15
2005	-7	-11	-5	-12	-7	-31	-12
2006	-6	-12	4	-8	-10	-32	-11
2007	-3	-10	-11	-10	-7	-28	-12
2008	-4	-10	-8	-11	-8	-28	-12
2009	0	-8	2	-5	-3	-27	-7
2010	-9	-16	-15	-18	-17	-35	-18
mean	-5	-10	-7	-11	-9	-31	-12

	CHIM	EMEP	LOTO	MATCH	MINNI	POLR	mean
2000	-2	-5	-6	-3	6	-2	-2
2001	-18	-21	-18	-18	-10	-22	-18
2002	-19	-25	-18	-21	-12	-26	-20
2003	-18	-20	-25	-16	-6	-25	-18
2004	-17	-23	-15	-16	-6	-23	-17
2005	-21	-24	-15	-17	-9	-22	-18
2006	-20	-24	-12	-16	-9	-25	-18
2007	-18	-25	-18	-16	-9	-22	-18
2008	-11	-17	-7	-6	1	-12	-9
2009	-7	-14	1	-4	6	-12	-5
2010	-17	-24	-14	-14	-10	-19	-16
mean	-15	-20	-13	-13	-5	-19	-14

Figure 1. Model biases (%) with respect to observations for PM₁₀ (left) and PM_{2.5} (right) for the period 2000-2010. Note: coarse sea salt is excluded in PM₁₀ from POLR.

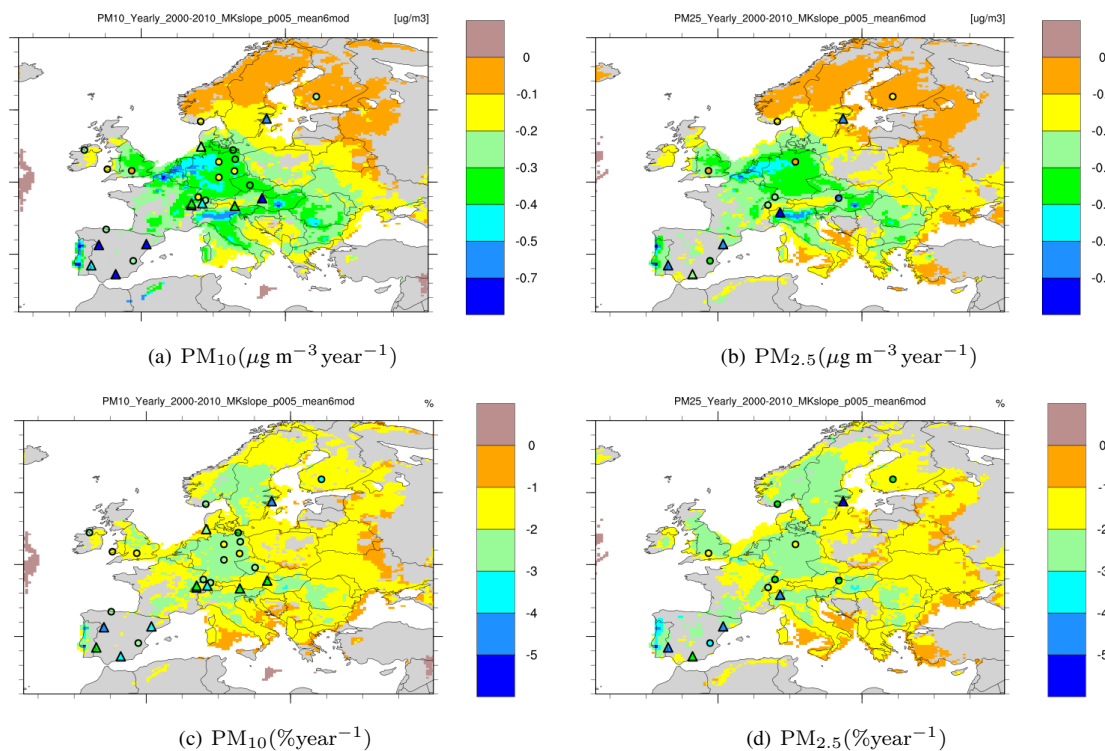


Figure 2. Mean Sen's slopes for PM_{10} and $\text{PM}_{2.5}$ trends in 2000-2010: absolute (a, b) and relative (c, d) slopes calculated by the 6-model ensemble (described in Colette et al. (2017a)), Appendix A3. Modelled trends – coloured contour map (grey or white means non-significant trends) and observed trends - coloured triangles (significant) and circles (non-significant).

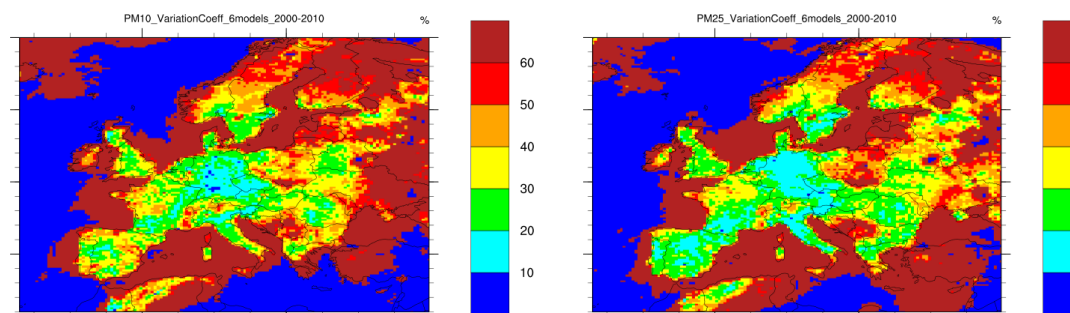


Figure 3. The Coefficient of Variation of PM_{10} (left) and $\text{PM}_{2.5}$ (right) trends simulated with the individual models relative to the 6-model ensemble mean for the period 2000-2010.

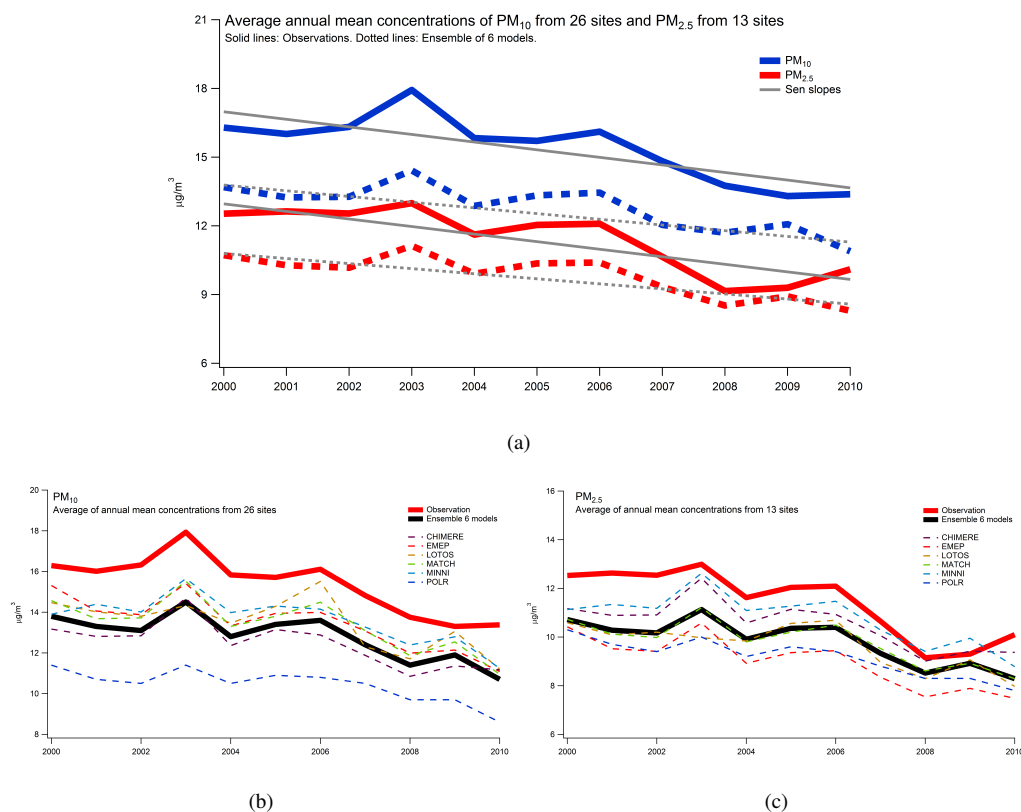


Figure 4. Observed and modelled (6-model ensemble) annual mean concentrations of PM₁₀ and PM_{2.5} and Sen's slopes (upper panel), averaged over the trend sites, for the period 2000–2010. Bottom figures also show results from the individual models (PM₁₀ from POLR does not include coarse sea salt). Note: gap filling of the missing years in the observations, mostly 2000 and 2001, was undertaken to ensure that the same set of sites was used throughout the whole period; see more details in the text.

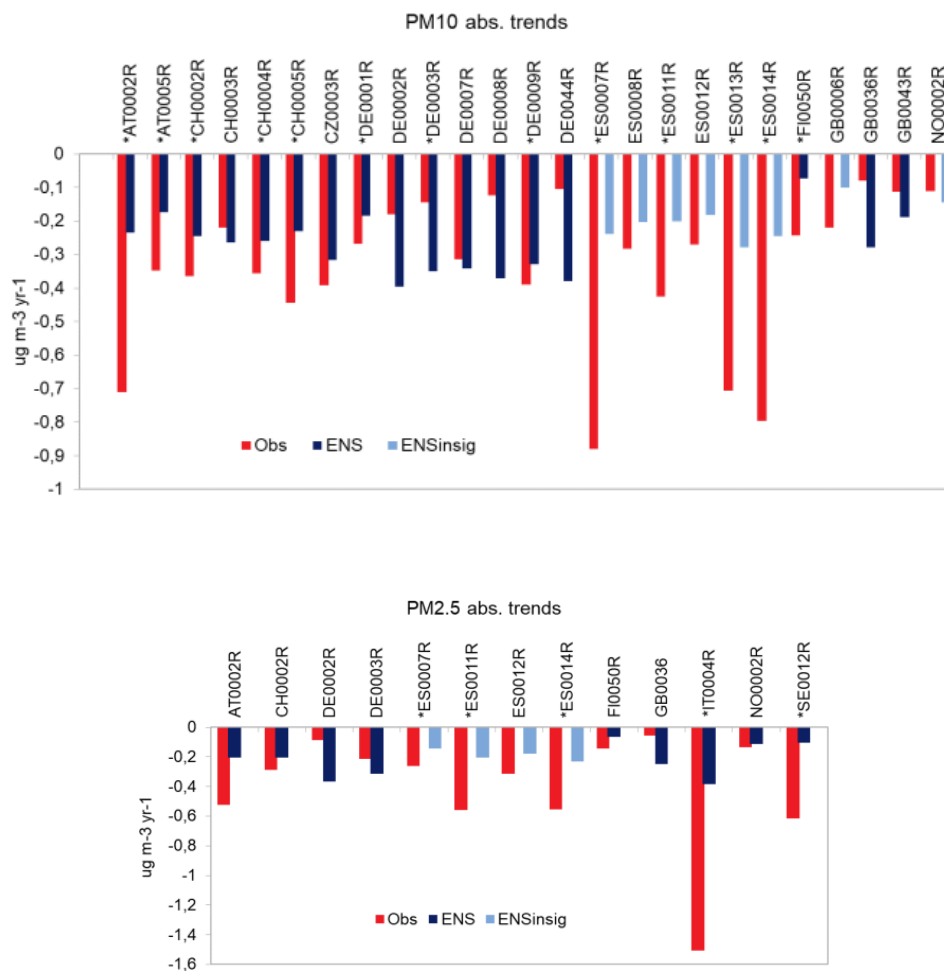


Figure 5. Observed and modelled (6-model ensemble) trend slopes ($\mu\text{g m}^{-3} \text{ year}^{-1}$) for the period 2000-2010 at the trend sites for PM_{10} (top) and $\text{PM}_{2.5}$ (bottom). Significant modelled trends are shown in dark blue, not-significant in light blue. Sites with significant observed trends are indicated by an asterisk.

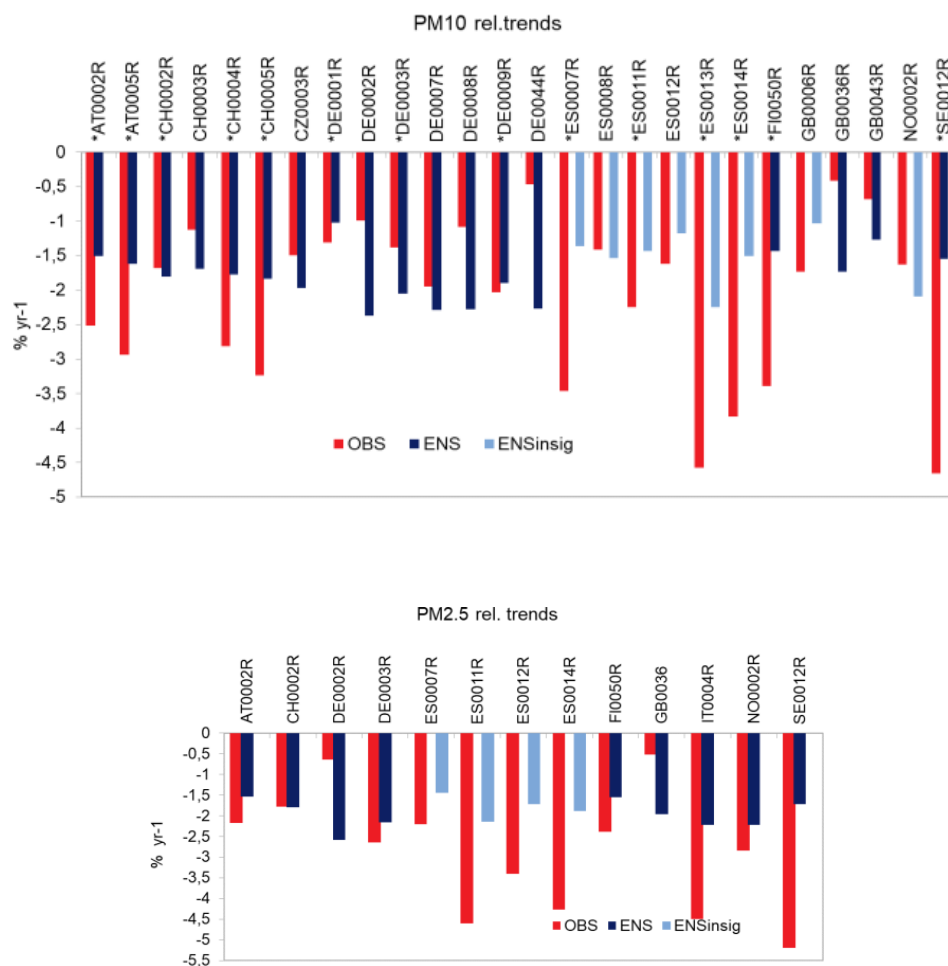


Figure 6. Same as Figure 5 for relative trends (% year⁻¹).

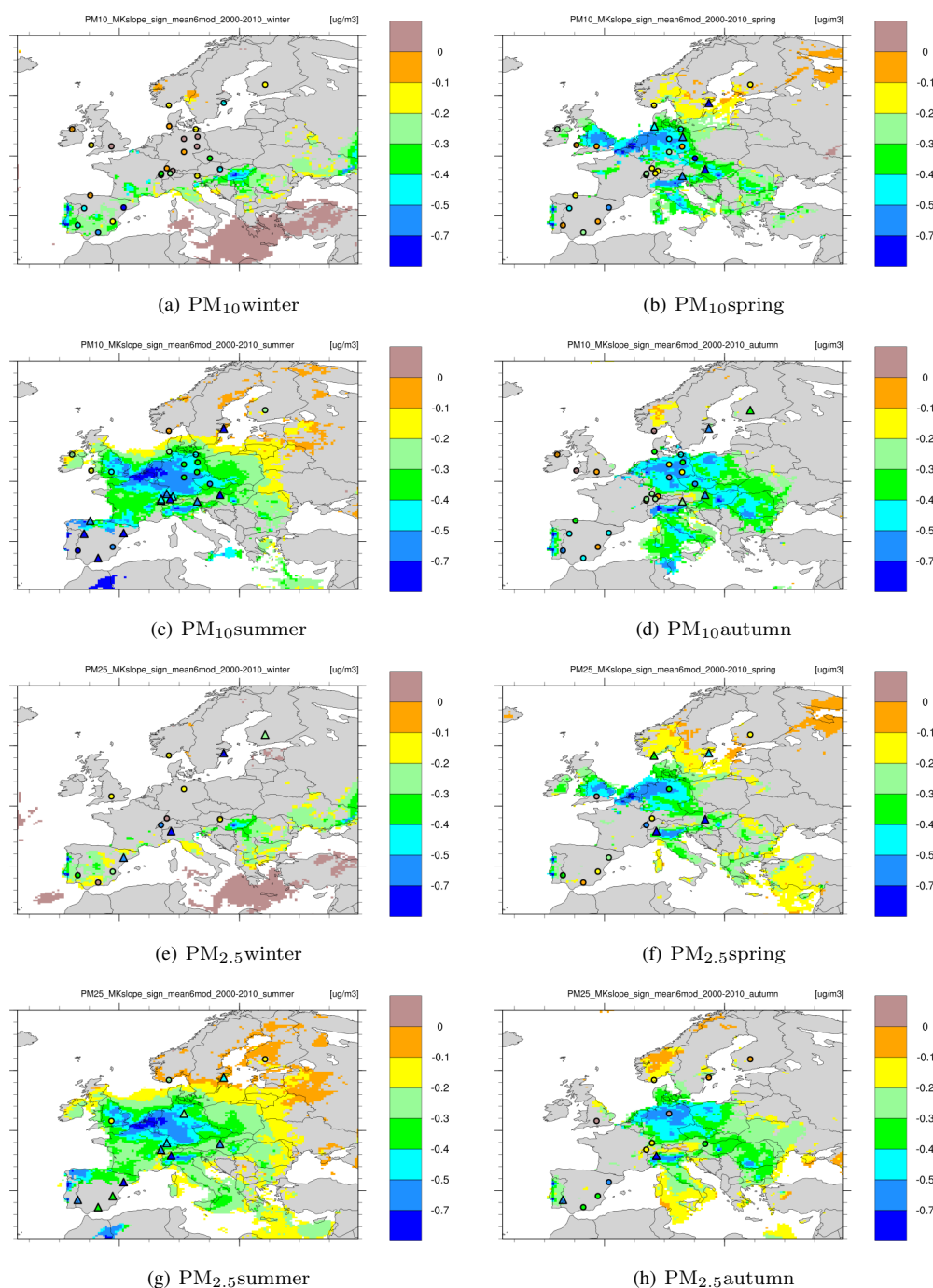


Figure 7. Mean Sen's slopes for PM₁₀ and PM_{2.5} seasonal trends for 2000-2010, calculated by the 6-model ensemble (see Figure 2 for explanation).

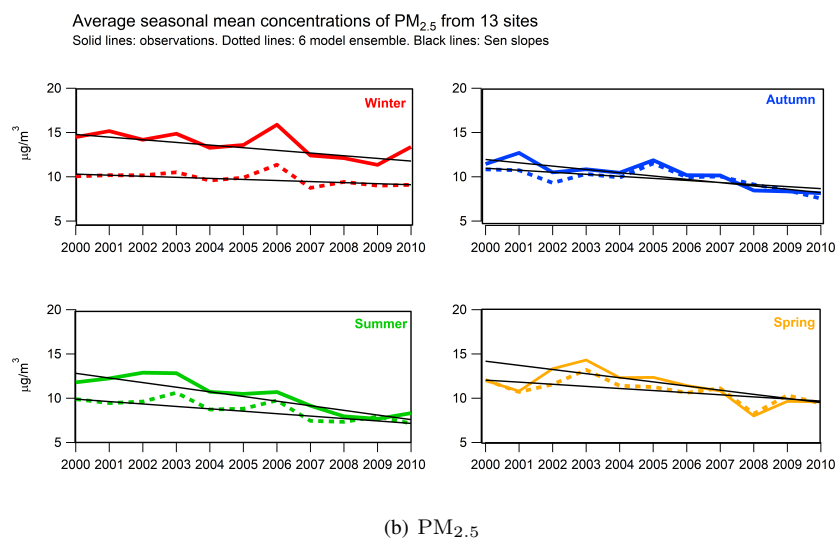
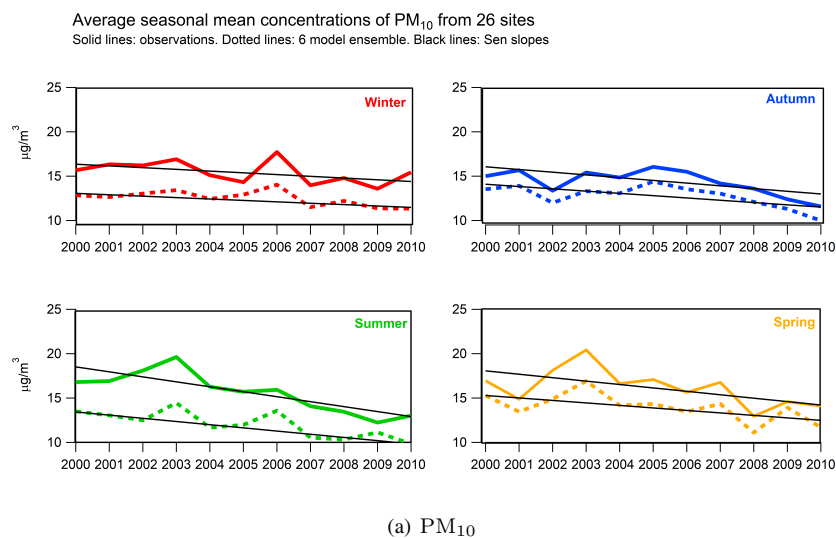


Figure 8. Changes in seasonal mean PM_{10} and $\text{PM}_{2.5}$ concentrations in the period 2000-2010, averaged over the trend-sites. Solid line: observed; Dashed line: 6-model ensemble.

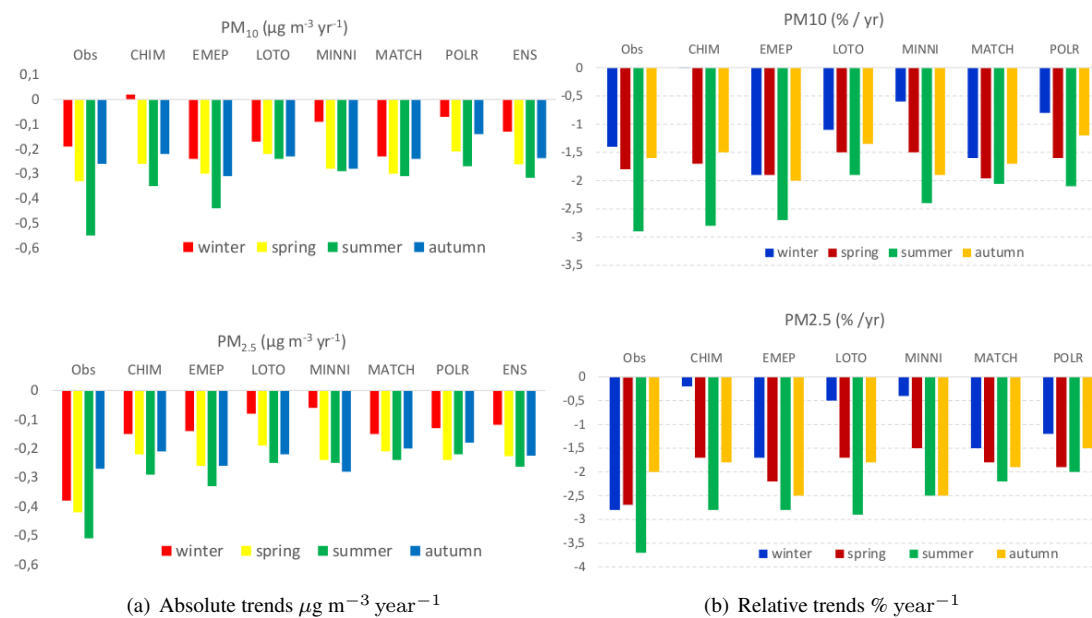


Figure 9. Mean relative seasonal trends in the period 2000-2010 at the trend-sites for PM_{10} and $\text{PM}_{2.5}$: The trends from the observations, the individual models and the 6-model ensemble are shown.

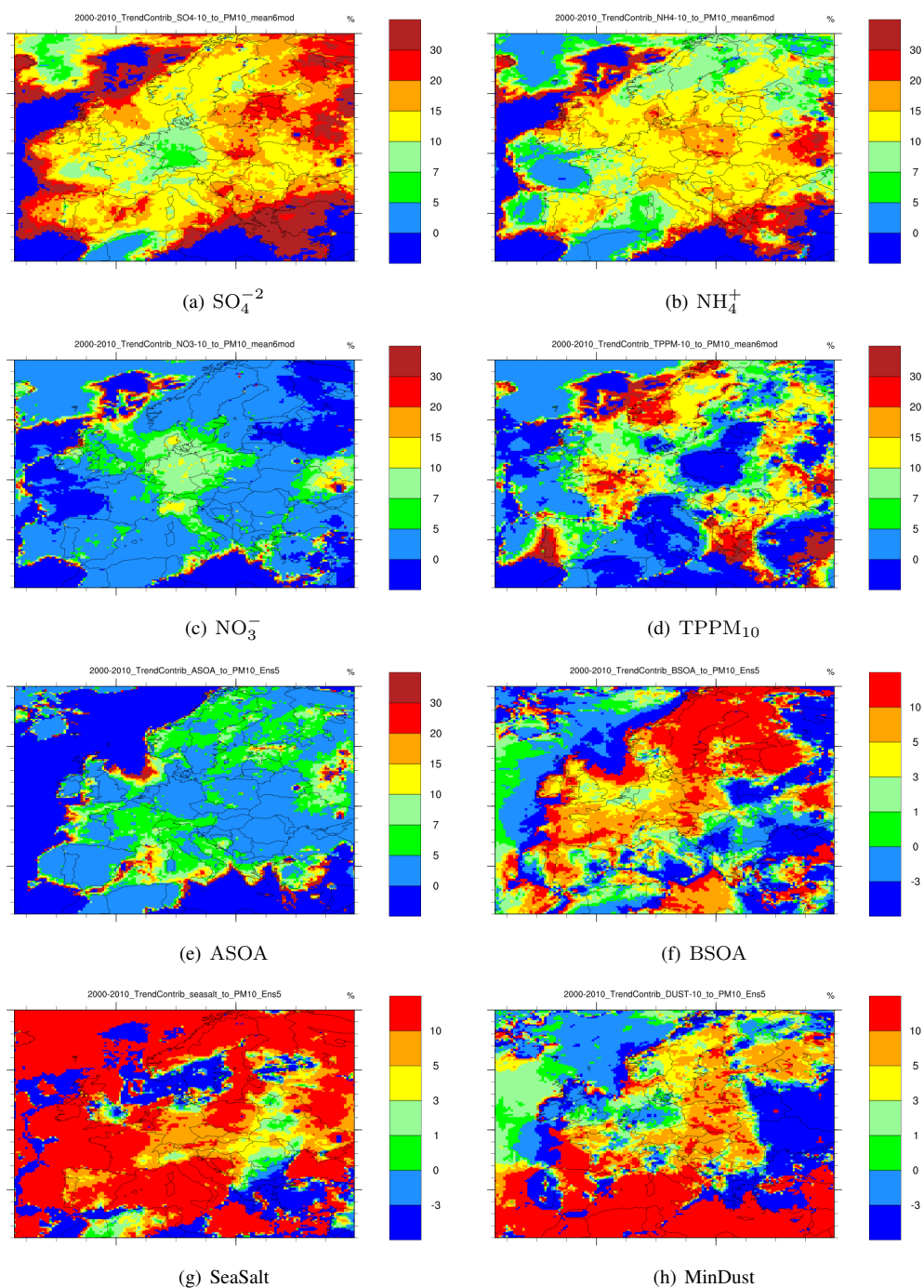


Figure 10. Model ensemble simulated relative contribution to PM₁₀ 2000-2010 trends from anthropogenic aerosols (all 6 models): SO_4^{2-} , NH_4^+ , NO_3^- , total primary TPPM₁₀ and anthropogenic SOA (except LOTO) and from natural aerosols: biogenic SOA (except LOTO), sea salt (except POLR) and mineral dust particles (except MATCH). Note that a different colour scale has been used for the natural aerosols.

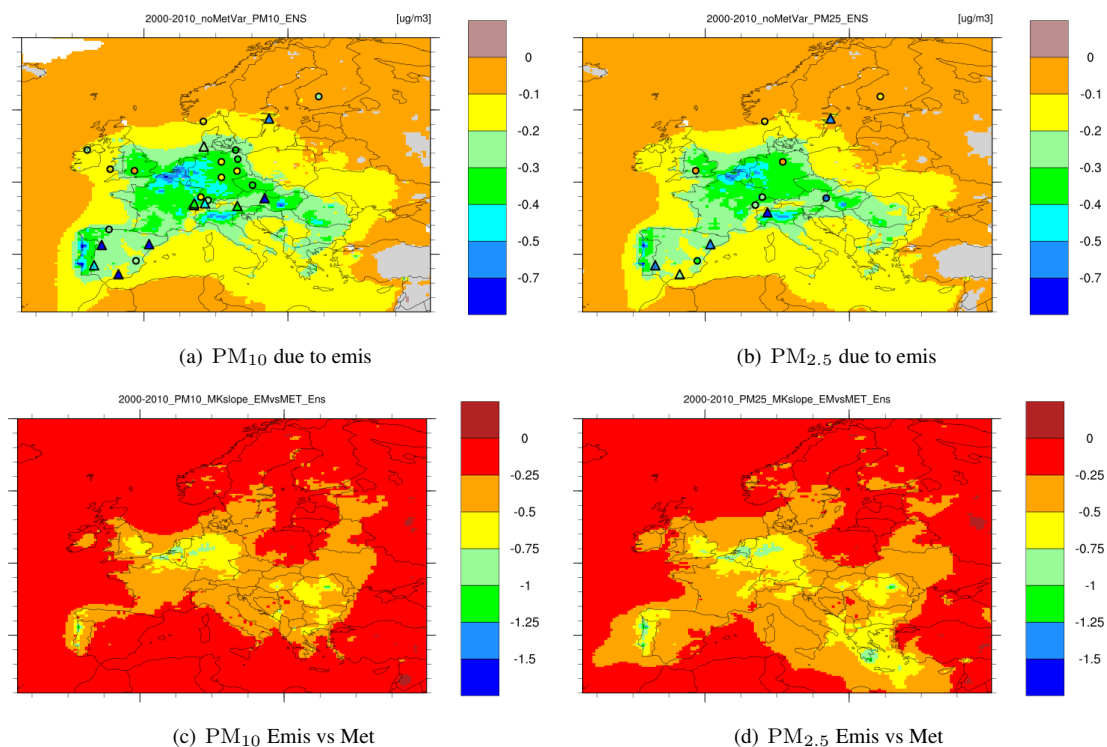


Figure 11. PM trends due to emission changes (upper panels) and the ratio of PM changes due to emission changes to those due to inter-annual meteorological variability (lower panels) for PM_{10} and $\text{PM}_{2.5}$ in the 2000-2010 period. Observed trends are shown as coloured triangles (significant) and circles (non-significant).



730 Appendix A: Supplementary Figures and Tables

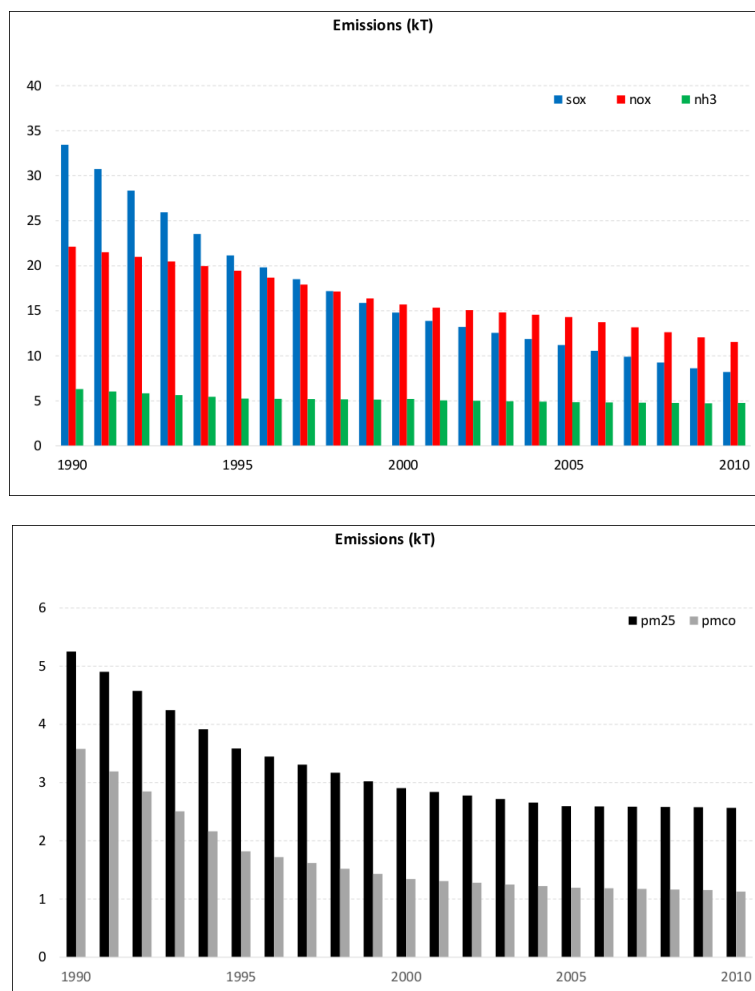


Figure A1. Annual emissions of SO_x, NO_x, NH₃, PM_{2.5} and PM coarse (pmco) in the period 1990-2010 (all countries). Units: ktonnes.

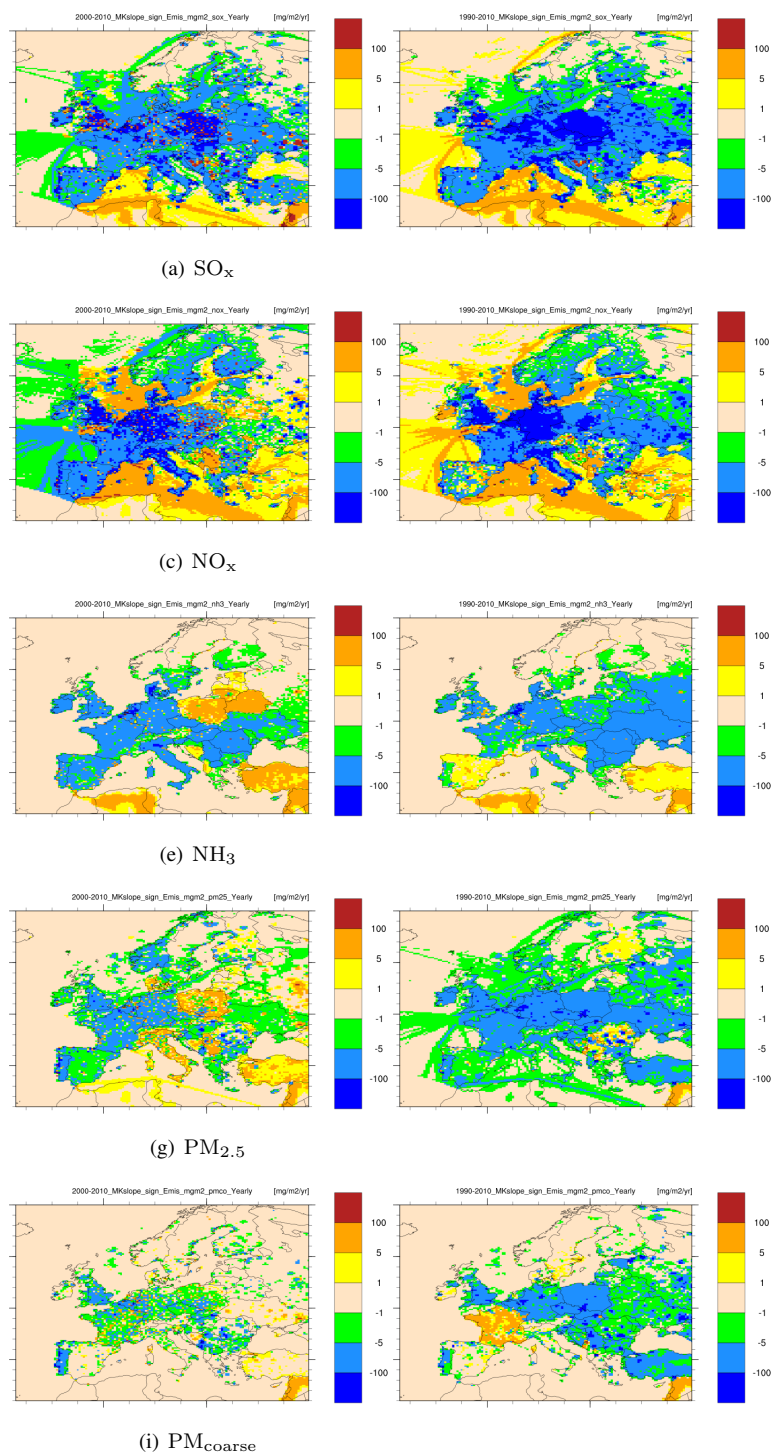


Figure A2. Emission trends for 2000-2010 (left) and 1990-2010 (right).

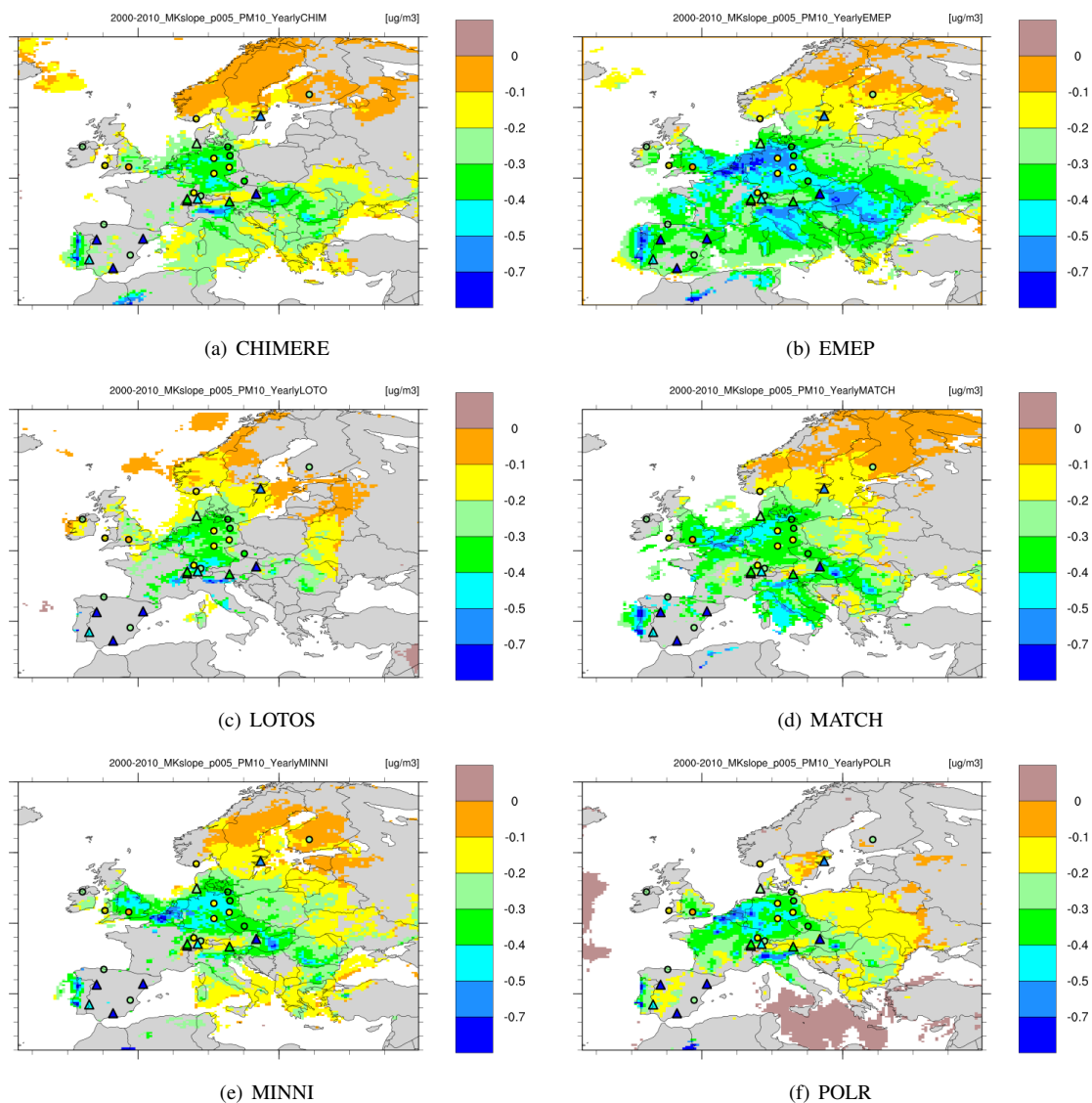


Figure A3. Annual mean trends (Sen's slopes) for PM_{10} in the period 2000-2010 as calculated by the individual models. The modelled trends are shown as coloured contour map (grey or white means non-significant trends) and the observed trends as coloured triangles (significant) and circles (non-significant). Units: $\mu g m^{-3} year^{-1}$.

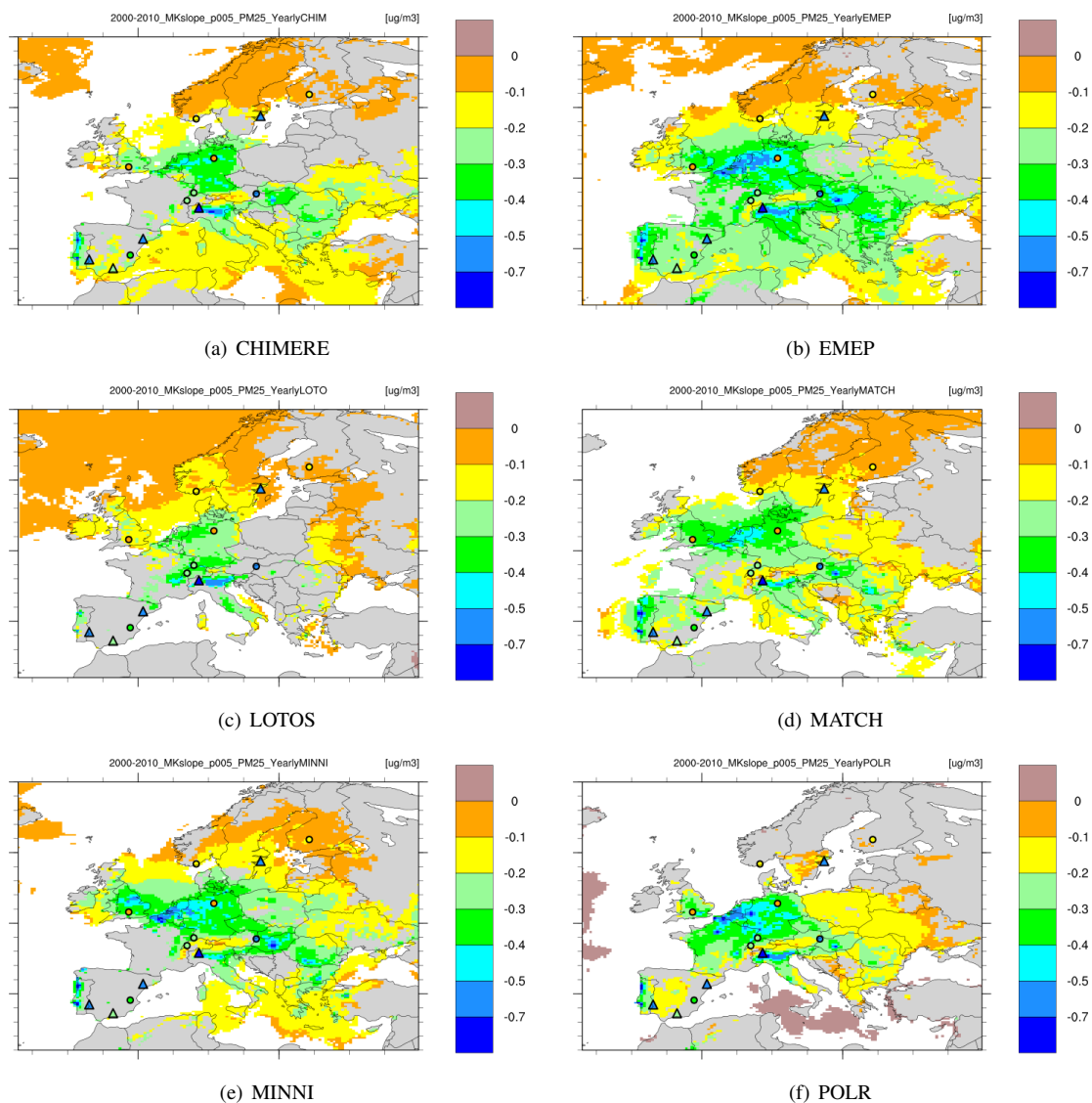


Figure A4. Same as Figure A3, but for $\text{PM}_{2.5}$. Units: $\mu\text{g m}^{-3} \text{ year}^{-1}$.

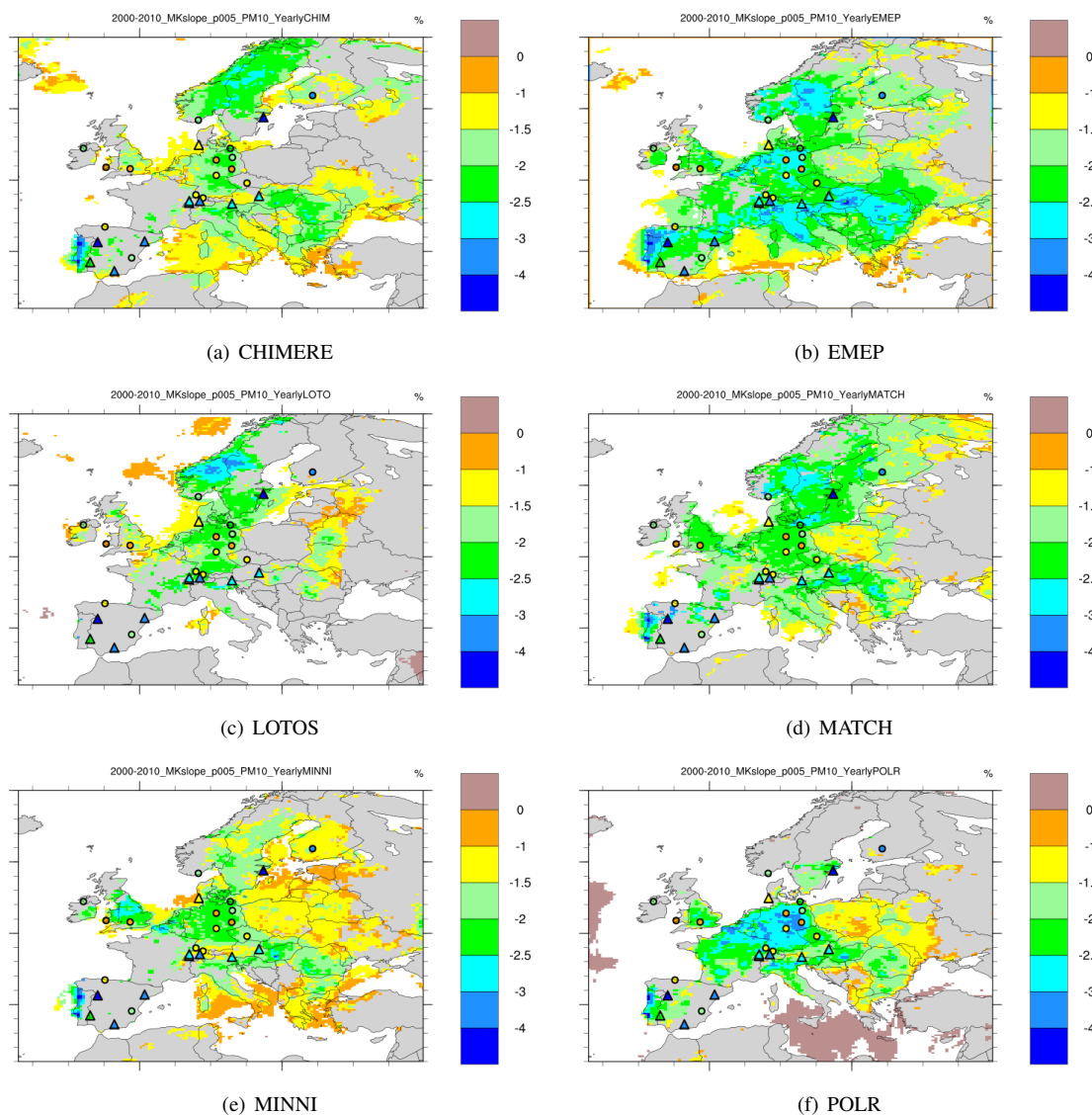


Figure A5. Mean Sen's slopes relative to the starting year of 2000 ($\% \text{ year}^{-1}$) for PM₁₀ trends in the period 2000-2010 calculated by the individual models. The modelled trends are shown as coloured contour map (grey or white means non-significant trends) and the observed trends as coloured triangles (significant) and circles (non-significant).

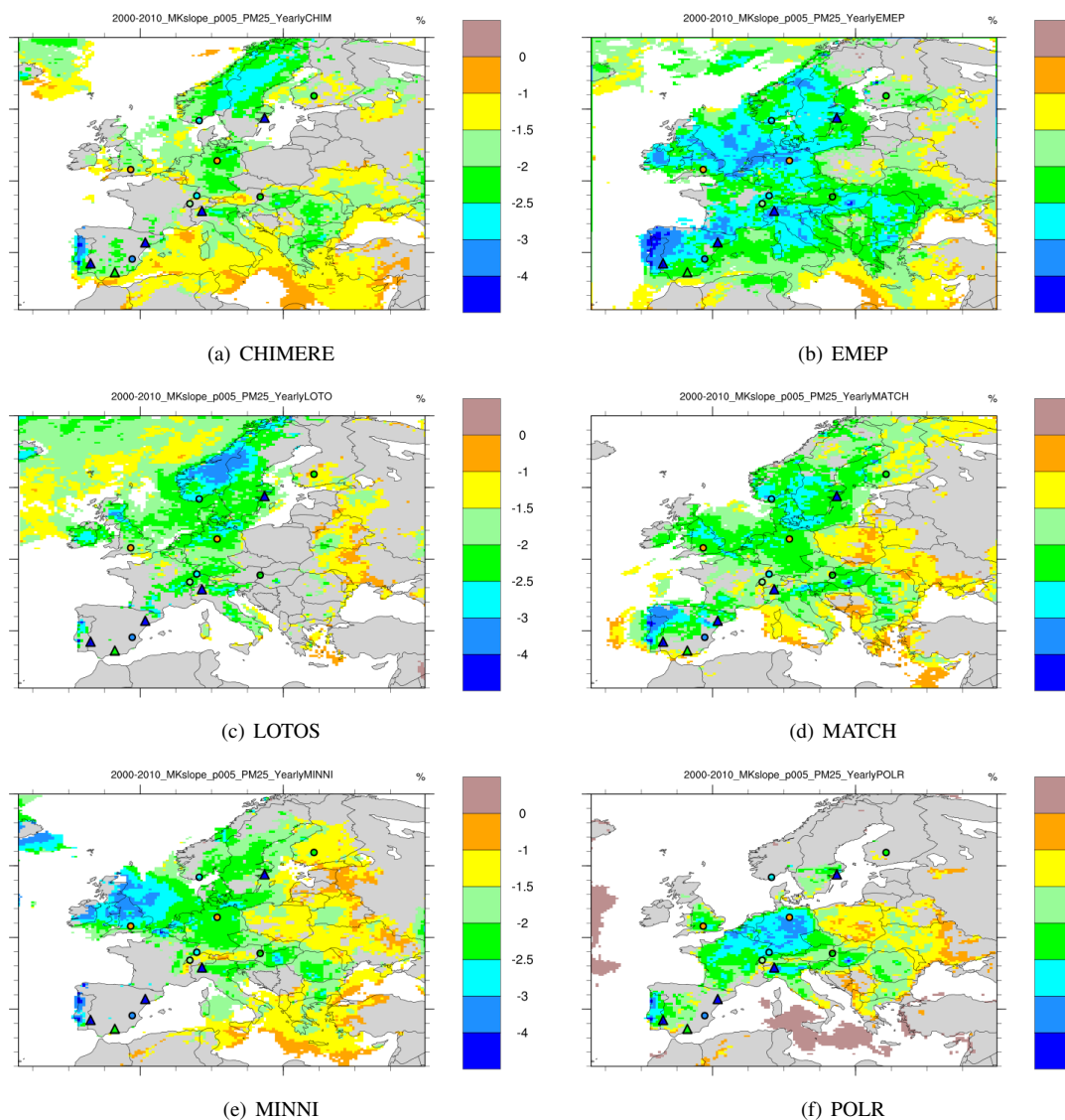


Figure A6. Same as Figure A5, but for $\text{PM}_{2.5}$. Units: $\% \text{ year}^{-1}$.

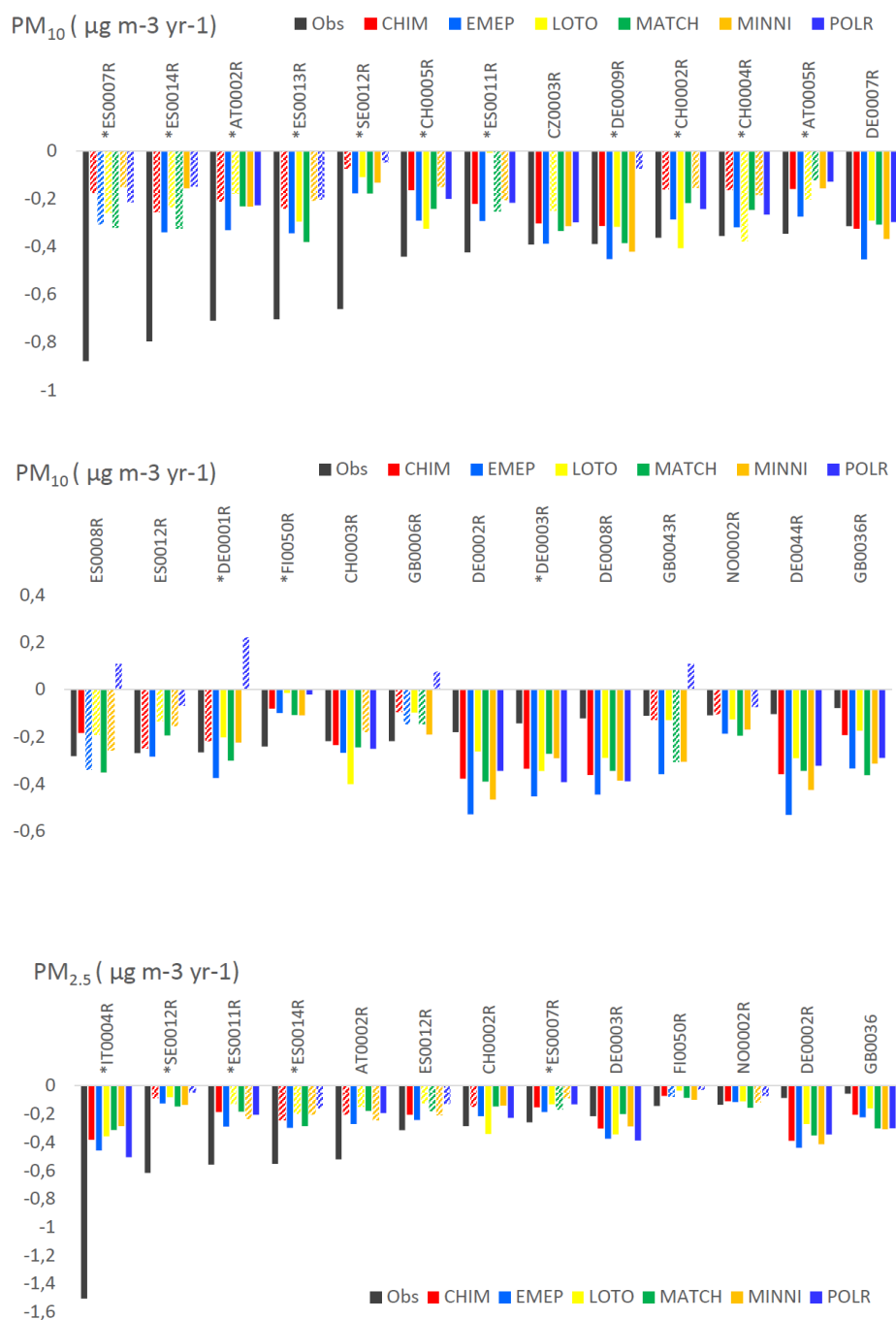


Figure A7. Observed and modelled trend slopes ($\mu\text{g m}^{-3} \text{ year}^{-1}$) for the period 2000-2010 at the trend sites: upper two plots for PM_{10} , lower plot for $\text{PM}_{2.5}$. The sites are sorted by decreasing observed negative trends and the sites at which significant trends were observed are marked with an asterisk and insignificant modelled trends are shown as striped bars. Units: $\mu\text{g m}^{-3} \text{ year}^{-1}$

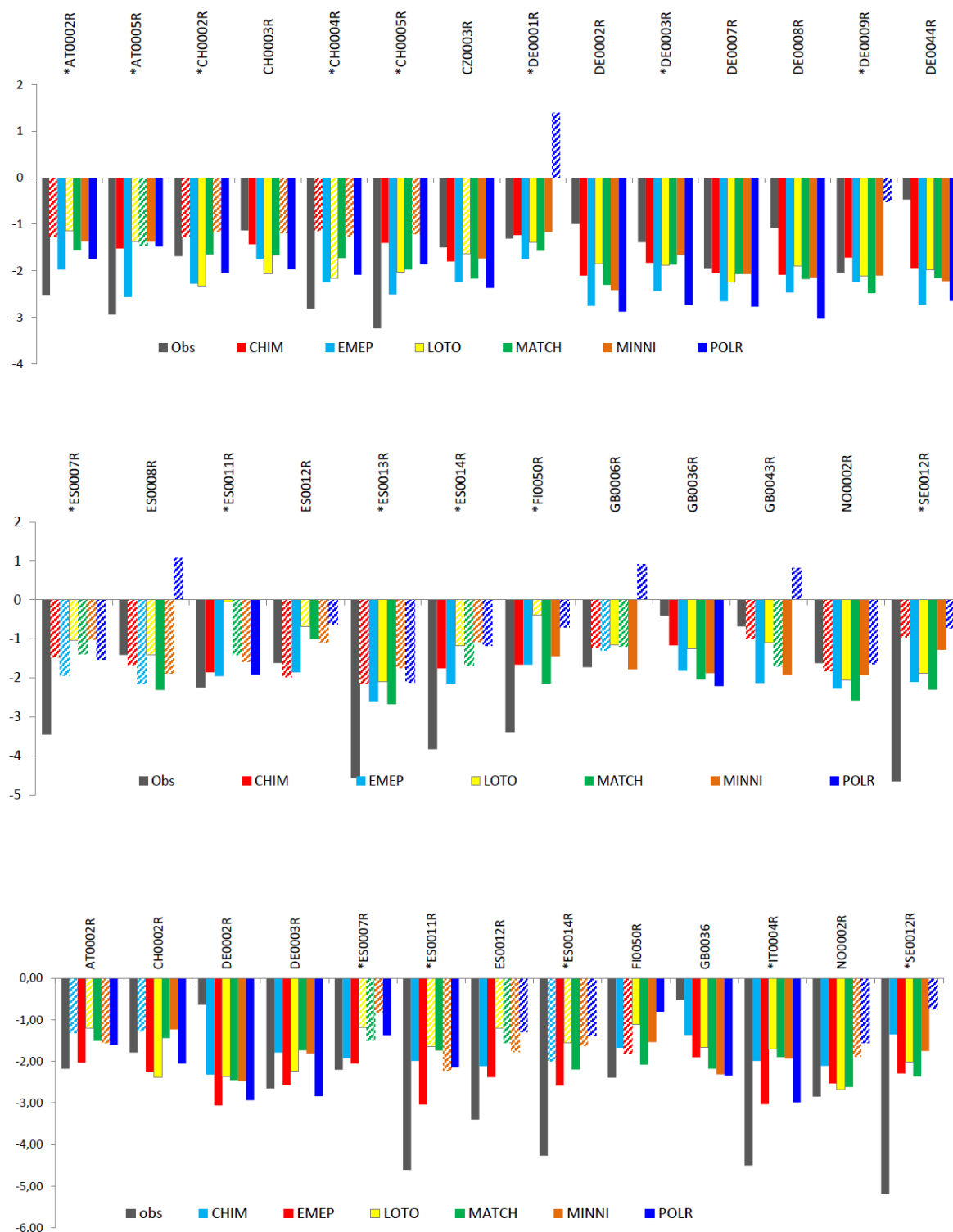


Figure A8. Mean observed (black) and modelled (coloured) relative trends for PM₁₀ (upper two graphs) and PM_{2.5} (lower graph) in the period 2000-2010 at the individual trend-sites. The sites at which significant trends were observed are marked with an asterisk and insignificant modelled trends are shown as striped bars. Units: % year⁻¹

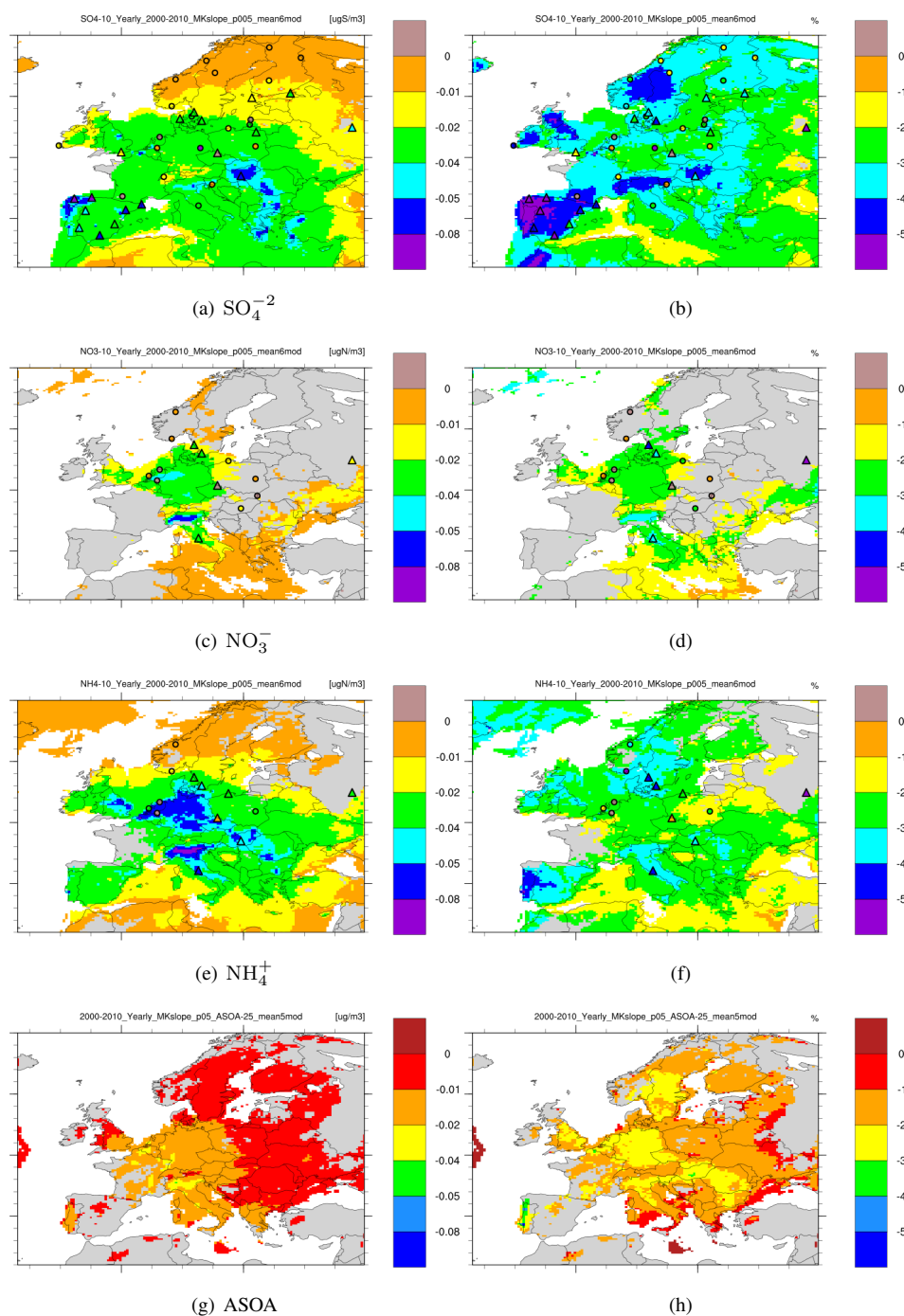


Figure A9. Mean observed and modelled Sen's trend slopes for 2000-2010 for anthropogenic aerosols: SO_4^{-2} , NO_3^- and NH_4^+ simulated by the 6-model ensemble (a-f) and for ASOA from the 5-model ensemble. Left panels – absolute ($\mu\text{g m}^{-3} (\text{S}) \text{ year}^{-1}$ and $\mu\text{g m}^{-3} (\text{N}) \text{ year}^{-1}$) and right panels – relative ($\% \text{ year}^{-1}$) trends. The modelled trends are shown as coloured contour map (grey or white means non-significant trends) and the observed trends as coloured triangles (significant) and circles (non-significant).

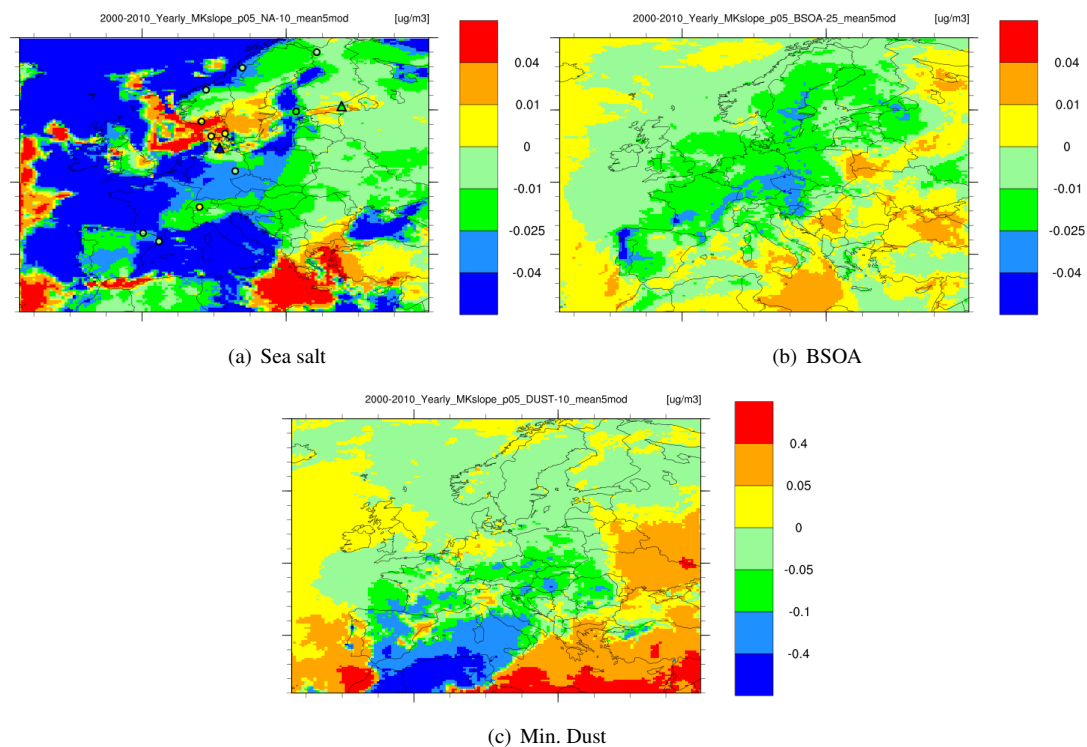


Figure A10. Mean Sen's trend slopes for 2000-2010 simulated by the 6-model ensemble for natural aerosols: (a) sea salt (observed trends also shown), (b) BSOA and (c) mineral dust. The modelled trends are shown as coloured contour map (grey or white means non-significant trends) and the observed trends as coloured triangles (significant) and circles (non-significant).

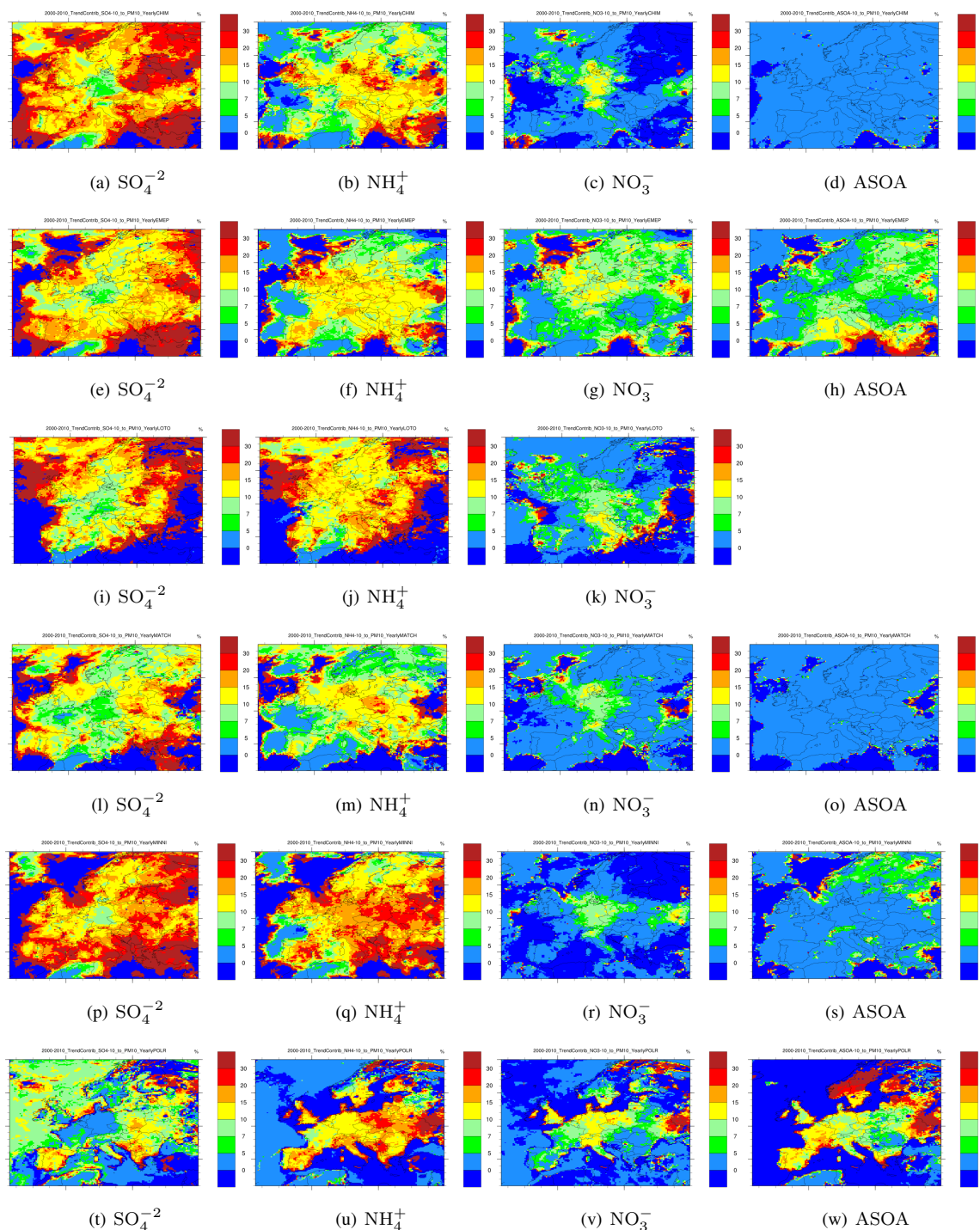


Figure A11. Relative contributions of (from left to right) SO₄⁻², NH₄⁺, NO₃⁻ and ASOA to PM₁₀ trends between 2000 and 2010 calculated by (from top to bottom) CHIMERE, EMEP, LOTOS-EUROS, MATCH, MINNI and Polair3D models.

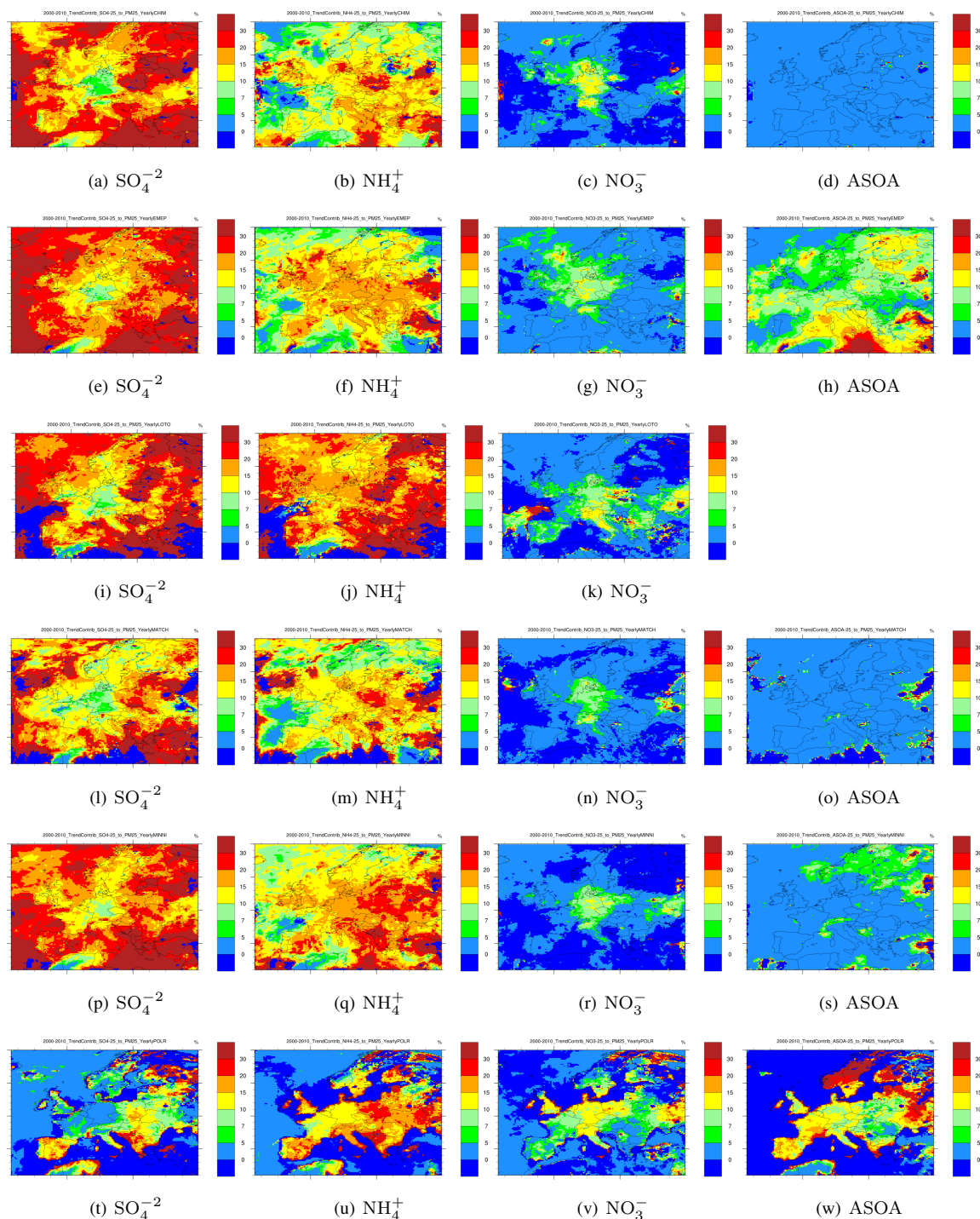


Figure A12. Relative contributions of (from left to right) SO_4^{2-} , NH_4^+ , NO_3^- and ASOA to $\text{PM}_{2.5}$ trends between 2000 and 2010 calculated by (from top to bottom) CHIMERE, EMEP, LOTOS-EUROS, MATCH, MINNI and Polair3D models.

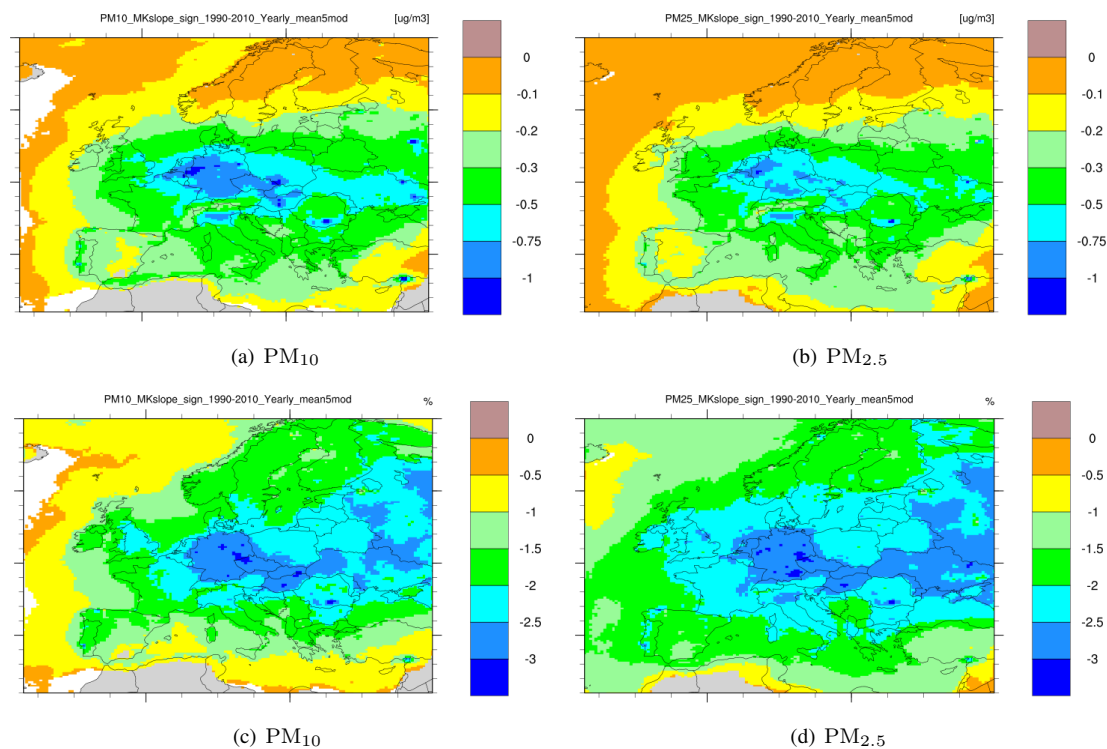


Figure A13. Annual mean Sen's slope for trends in the period 1990-2010 as calculated by the 6-model ensemble (left) for PM₁₀ and (right) PM_{2.5}. Upper panels – absolute ($\mu\text{g m}^{-3} \text{ year}^{-1}$) and lower panels – relative to 1990 ($\% \text{ year}^{-1}$).

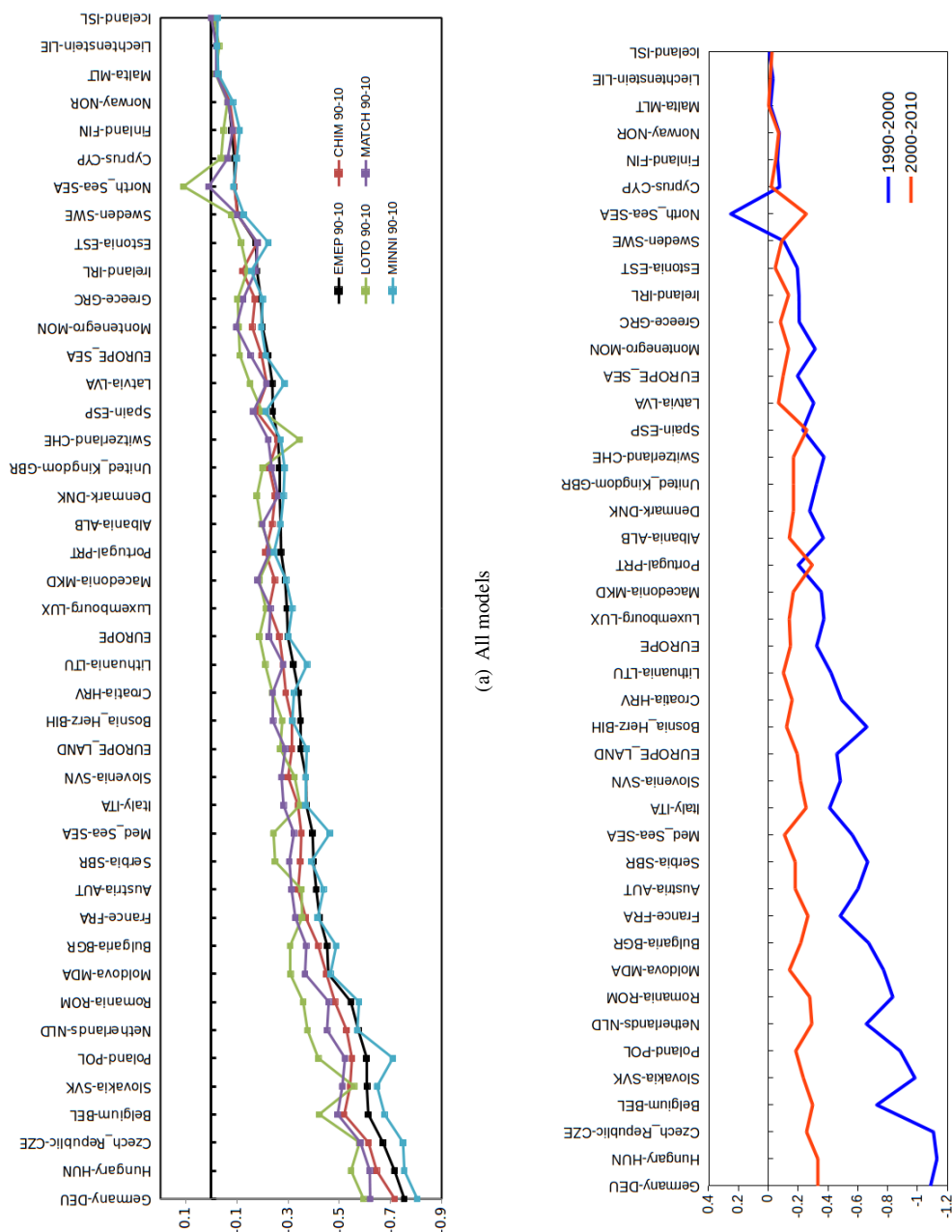


Figure A14. Modelled PM_{10} trends calculated for European countries ($\mu g m^{-3} year^{-1}$): a. the individual models for the period 1990-2010, and b. the model ensemble for the periods 1990-2000 and 2000-2010 separately. The countries are ranged according to descending 1990-2010 negative trends from the EMEP model (a).

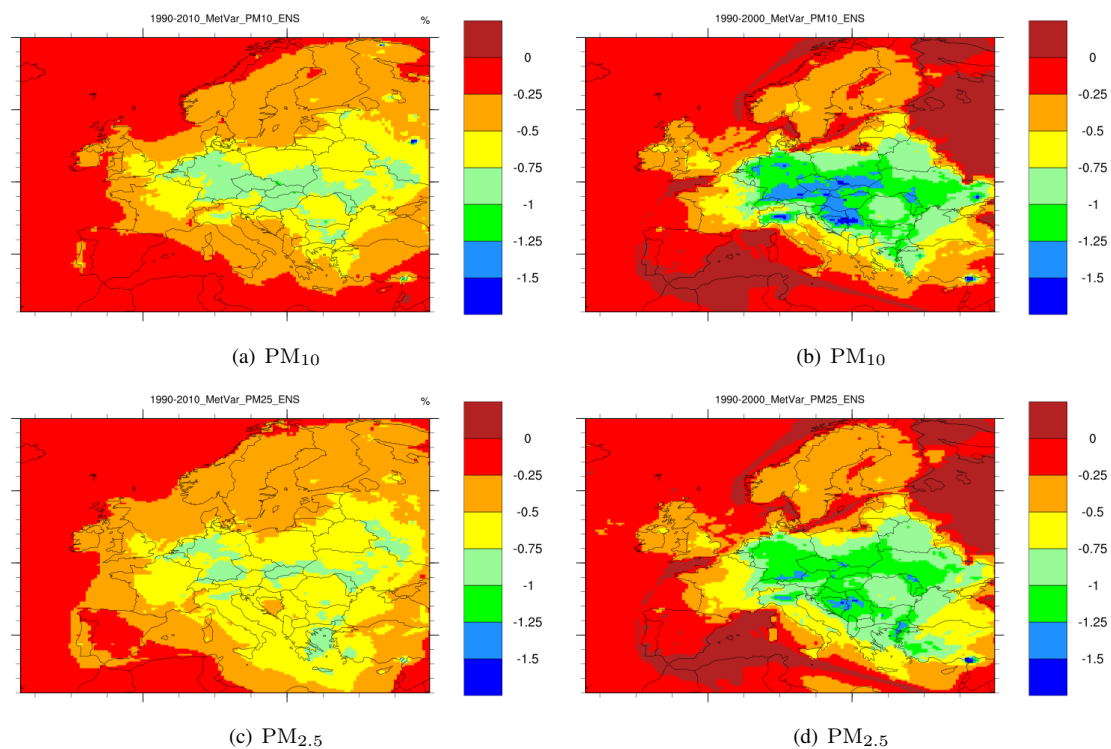


Figure A15. The ratio of PM changes due to emission changes to those due to inter-annual meteorological variability for PM₁₀ and PM_{2.5} for 1990-2010 (left panels) and 1990-2000 (right panels) periods.



Competing interests. No competing interest are present.

Acknowledgements. The Ineris coordination of the EURODELTA-Trends exercise was supported by the French Ministry in charge of Ecology in the context of the Task Force on Measurement and Modelling of the EMEP program of the LRTAP Convention. Meteorological forcing with the WRF model was provided by Robert Vautard and Annemiek Stegehuis from LSCE/IPSL. The CHIMERE simulations were performed using the TGCC supercomputers under GENCI computing allocation. The participation of CIEMAT was financed by the Spanish Ministry of Agriculture and Fishing, Food and Environment.

Computer time for EMEP model runs was supported by the Research Council of Norway through the NOTUR project EMEP (NN2890K) for CPU and the NorStore project European Monitoring and Evaluation Programme (NS9005K) for storage of data.

Funding for the MATCH participation was jointly divided between Nordforsk through the research programme Nordic Welfair (grant no 75007), the Swedish Environmental Protection Agency through the SCAC research programme and the 2017-2018 Belmont Forum and BiodivERsA joint call for research proposals, under the BiodivScen ERA-Net COFUND programme, with the funding organisations AKA (contract no 326328), ANR (ANR-18-EBI4-007), BMBF (KFZ: 01LC1810A), FORMAS (contract no's: 2018-02434, 2018-02436, 2018-02437, 2018-02438) and MICINN (APCIN; PCI2018-093149).

LOTOS-team thanks Erik van Meijgaard of the Royal Netherlands Meteorological Institute (KNMI) for providing the RACMO2 simulations that were used by LOTOS-EUROS.

The computing resources and the related technical support used for MINNI simulations have been provided by CRESCO/ENEAGRID High Performance Computing infrastructure and its staff. The infrastructure is funded by ENEA, the Italian National Agency for New Technologies, Energy and Sustainable Economic Development and by Italian and European research programmes (<http://www.cresco.enea.it/english>, last access: 21 December 2018). MINNI participation to this project was supported by the “Cooperation Agreement for support to international Conventions, Protocols and related negotiations on air pollution issues”, funded by the Italian Ministry for the Environment, Land and Sea.

CIEMAT acknowledges the Ministry for the Ecological Transition and Demographic Challenge (MITERD) for financial support.

The GAINS emission trends were produced as part of the FP7 European Research Project ECLIPSE (Evaluating the Climate and Air Quality Impacts of Short-Lived Pollutants) grant no. 282688.



Table A1. Selected set of EMEP monitoring stations for PM₁₀ and PM_{2.5} trend analysis for the period 2000–2010

Sites Code	Name	latitude	longitude	altitude	PM ₁₀ measurements			PM _{2.5} measurements		
					Sampler	Frequency	Nr of years	Sampler	Frequency	Nr of years
AT0002R	Illmitz	47.767	16.767	117.0m	high vol	daily	11	high vol	daily	10
AT0005R	Vorhegg	46.678	12.972	1020.0m	high vol	daily	10			
CH0002R	Payerne	46.813	6.945	489.0m	high vol	daily	11	high vol	daily	11
CH0003R	Tänikon	47.480	8.905	539.0m	high vol	daily	11			
CH0004R	Chaumont	47.050	6.979	1137.0m	high vol	daily	11			
CH0005R	Rigi	47.068	8.464	1031.0m	high vol	daily	11			
CZ0003R	Kosetice (NOAK)	49.573	15.080	535.0m	b-attenuation ¹	hourly	10			
DE0001R	Westerland	54.926	8.310	12.0m	high vol	daily	11			
DE0002R	Waldhof	52.802	10.759	74.0m	high vol	daily	11	high vol	daily	11
DE0003R	Schauinsland	47.915	7.909	1205.0m	high vol	daily	11	high vol	daily	10
DE0007R	Neuglobsow	53.167	13.033	62.0m	high vol	daily	11			
DE0008R	Schmütke	50.650	10.767	937.0m	high vol	daily	11			
DE0009R	Zingst	54.437	12.725	1.0m	high vol	daily	11			
DE0044R	Melpitz	51.530	12.934	86.0m	high vol	daily	11			
ES0007R	Viznar	37.233	-3.533	1265.0m	high vol	daily	10	high vol	daily	10
ES0008R	Niembro	43.442	-4.850	134.0m	high vol	daily	10			
ES0011R	Barcarrota	38.476	-6.923	393.0m	high vol	daily	10	high vol	daily	10
ES0012R	Zarra	39.086	-1.102	885.0m	high vol	daily	10	high vol	daily	10
ES0013R	Penausende	41.283	-5.867	985.0m	high vol	daily	10			
ES0014R	Els Torms	41.400	0.717	470.0m	high vol	daily	10	high vol	daily	10
FI0050R	Hyttälä	61.850	24.283	181.0m	low vol ³	daily	11	low vol ³	daily	11
GB0006R	Lough Navar	54.443	-7.870	126.0m	TEOM FDMS	daily	11	TEOM FDMS	hourly	11
GB0036R	Harwell	51.573	-1.317	137.0m	TEOM FDMS	daily	11			
GB0043R	Narberth	51.782	-4.691	160.0m	TEOM FDMS	daily	9	TEOM	hourly	10
IT0004R	Ispra	45.800	8.633	209.0m	low vol	weekly	11	low vol	daily	10
NO0002R	Birkenes II	58.389	8.252	219.0m	b-attenuation ²	daily	10	low vol	weekly	10
SE0012R	Aspvreten	58.800	17.383	20.0m				TEOM	hourly	10

¹ Thermo FH 62 I-R, ² OPSIS SM200, ³ with 4 stage cascade impactor



Table A2. Relative bias and correlation for modelled PM₁₀ with respect to observations at 26 sites for the years 2000 to 2010

Year		CHIM		EMEP		LOTO		MATCH		MINNI		POLR*	
	Nsite	Bias	Corr	Bias	Corr	Bias	Corr	Bias	Corr	Bias	Corr	Bias	Corr
2000	15	-2	0.64	2	0.58	-6	0.47	-11	0.60	-4	0.58	-24	0.62
2001	21	-4	0.41	-8	0.61	-4	0.60	-9	0.71	-8	0.48	-30	0.59
2002	22	-7	0.55	-14	0.60	-13	0.46	-16	0.63	-14	0.61	-35	0.60
2003	22	-8	0.59	-13	0.63	-16	0.40	-12	0.55	-12	0.63	-36	0.64
2004	22	-7	0.50	-14	0.64	-10	0.66	-14	0.78	-9	0.60	-33	0.64
2005	23	-7	0.55	-11	0.63	-5	0.51	-12	0.65	-7	0.62	-31	0.65
2006	21	-6	0.48	-12	0.48	4	0.24	-8	0.34	-10	0.52	-32	0.42
2007	21	-3	0.39	-10	0.50	-11	0.43	-10	0.61	-7	0.48	-28	0.50
2008	21	-4	0.37	-10	0.49	-8	0.44	-11	0.63	-8	0.48	-28	0.53
2009	22	0	0.53	-8	0.61	2	0.39	-5	0.50	-3	0.59	-27	0.57
2010	21	-9	0.58	-16	0.62	-15	0.23	-18	0.46	-17	0.60	-35	0.53

Bias - relative bias i %, Corr - spatial correlation with observations over the sites.

* Excluding coarse sea salt

Table A3. Relative bias and correlation for modelled PM_{2.5} with respect to observations at 26 sites for the years 2000 to 2010

Year		CHIM		EMEP		LOTO		MATCH		MINNI		POLR	
	Nsite	Bias	Corr	Bias	Corr	Bias	Corr	Bias	Corr	Bias	Corr	Bias	Corr
2000	7	-2	0.71	-5	0.63	-6	0.69	-3	0.64	6	0.71	-2	0.69
2001	12	-18	0.59	-21	0.61	-18	0.79	-18	0.70	-10	0.53	-22	0.73
2002	12	-19	0.64	-25	0.68	-18	0.73	-21	0.70	-12	0.60	-26	0.72
2003	12	-18	0.74	-20	0.72	-25	0.70	-16	0.69	-6	0.70	-25	0.74
2004	12	-17	0.61	-23	0.62	-15	0.77	-16	0.73	-6	0.54	-23	0.72
2005	13	-21	0.68	-24	0.63	-15	0.73	-17	0.69	-9	0.59	-22	0.74
2006	11	-20	0.69	-24	0.50	-12	0.65	-16	0.55	-9	0.45	-25	0.61
2007	11	-18	0.59	-25	0.52	-18	0.63	-16	0.73	-9	0.40	-22	0.69
2008	11	-11	0.60	-17	0.60	-7	0.71	-6	0.69	1	0.54	-12	0.71
2009	11	-7	0.65	-14	0.61	1	0.76	-4	0.64	6	0.57	-12	0.67
2010	10	-17	0.62	-24	0.58	-14	0.68	-14	0.66	-10	0.64	-19	0.67

Bias - relative bias i %, Corr - spatial correlation with observations over the sites



755 References

- Air quality in Europe — 2020 report, EEA Report No 09/2020, ISSN 1977-8449, European Environment Agency, Copenhagen, <https://doi.org/10.2800/786656>, 2009.
- Aas, W., Mortier, A., Bowersox, V., Cherian, R., Faluvegi, G., Fagerli, H., Hand, J., Klimont, Z., Galy-Lacaux, C., Lehmann, C. M., et al.: Global and regional trends of atmospheric sulfur, *Scientific reports*, 9, 1–11, 2019.
- 760 Aas, W., Fagerli, H., Yttri, K. E., Tsyro, S., Solberg, S., Simpson, D., Gliß, J., Mortier, A., Grøtting Wærsted, E., Brenna, H., Hjellbrekke, A., Griesfeller, J., Nyíri, A., Gauss, M., and Scheuschner, T.: Trends in observations and EMEP MSC-W model calculations 2000–2019, in: *Transboundary particulate matter, photo-oxidants, acidifying and eutrophying components*. EMEP Status Report 1/2021, pp. 83–97, The Norwegian Meteorological Institute, Oslo, Norway, 2021.
- Amann, M.: Future emissions of air pollutants in Europe–Current legislation baseline and the scope for further reductions, <http://pure.iiasa.ac.at/id/eprint/10164/1/XO-12-011.pdf>, 2012.
- 765 Amann, M., Bertok, I., Borken-Kleefeld, J., Cofala, J., Heyes, C., Höglund-Isaksson, L., Klimont, Z., Nguyen, B., Posch, M., Rafaj, P., et al.: Cost-effective control of air quality and greenhouse gases in Europe: Modeling and policy applications, *Environmental Modelling & Software*, 26, 1489–1501, 2011.
- Barmapadimos, I., Keller, J., Oderbolz, D., Hueglin, C., and Prévôt, A. S. H.: One decade of parallel fine ($\text{PM}_{2.5}$) and coarse
 770 ($\text{PM}_{10}-\text{PM}_{2.5}$) particulate matter measurements in Europe: trends and variability, *Atmospheric Chemistry and Physics*, 12, 3189–3203, <https://doi.org/10.5194/acp-12-3189-2012>, <https://www.atmos-chem-phys.net/12/3189/2012/>, 2012.
- Bergström, R., Hallquist, M., Simpson, D., Wildt, J., and Mentel, T. F.: Biotic stress: a significant contributor to organic aerosol in Europe?, *Atmospheric Chemistry and Physics*, 14, 13 643–13 660, <https://doi.org/10.5194/acp-14-13643-2014>, <http://www.atmos-chem-phys.net/14/13643/2014/>, 2014.
- 775 Bessagnet, B., Pirovano, G., Mircea, M., Cuvelier, C., Aulinger, A., Calori, G., Ciarelli, G., Manders, A., Stern, R., Tsyro, S., and et al.: Presentation of the EURODELTA III intercomparison exercise – evaluation of the chemistry transport models’ performance on criteria pollutants and joint analysis with meteorology, *Atmospheric Chemistry and Physics*, 16, 12 667–12 701, <https://doi.org/10.5194/acp-16-12667-2016>, 2016.
- Ciarelli, G., Theobald, M. R., Vivanco, M. G., Beekmann, M., Aas, W., Andersson, C., Bergström, R., Manders-Groot, A., Couvidat, F.,
 780 Mircea, M., et al.: Trends of inorganic and organic aerosols and precursor gases in Europe: insights from the EURODELTA multi-model experiment over the 1990–2010 period, *Geoscientific Model Development*, 12, 4923–4954, 2019.
- Colette, A., Granier, C., Hodnebrog, Ø., Jacobs, H., Maurizi, A., Nyíri, A., Bessagnet, B., D’Angiola, A., D’Isidoro, M., Gauss, M., Meleux, F., Memmesheimer, M., Mieville, A., Rouïl, L., Russo, F., Solberg, S., Stordal, F., and Tampieri, F.: Air quality trends in Europe over the past decade: a first multi-model assessment, *Atmos. Chem. Phys.*, 11, 11 657–11 678, <https://doi.org/10.5194/acp-11-11657-2011>,
 785 <https://www.atmos-chem-phys.net/11/11657/2011/>, 2011.
- Colette, A., Aas, W., Banin, L., Braban, C., Ferm, M., González Ortiz, A., Ilyin, I., Mar, K., Pandolfi, M., Putaud, J.-P., Shatalov, V., Solberg, S., Spindler, G., Tarasova, O., Vana, M., Adani, M., Almodovar, P., Berton, E., Bessagnet, B., Bohlin-Nizzetto, P., Boruvkova, J., Breivik, K., Briganti, G., Cappelletti, A., Cuvelier, K., Derwent, R., D’Isidoro, M., Fagerli, H., Funk, C., Garcia Vivanco, M., González Ortiz, A., Haeuber, R., Hueglin, C., Jenkins, S., Kerr, J., de Leeuw, F., Lynch, J., Manders, A., Mircea, M., Pay, M., Pritula, D., Putaud, J.-P.,
 790 Querol, X., Raffort, V., Reiss, I., Roustan, Y., Sauvage, S., Scavo, K., Simpson, D., Smith, R., Tang, Y., Theobald, M., Tørseth, K., Tsyro, S., van Pul, A., Vidic, S., Wallasch, M., and Wind, P.: Air Pollution trends in the EMEP region between 1990 and 2012., *Tech. Rep.*



- Joint Report of the EMEP Task Force on Measurements and Modelling (TFMM), Chemical Co-ordinating Centre (CCC), Meteorological
 Synthesizing Centre-East (MSC-E), Meteorological Synthesizing Centre-West (MSC-W) EMEP/CCC Report 1/2016, Norwegian Institute
 for Air Research, Kjeller, Norway, [http://www.unece.org/fileadmin/DAM/env/documents/2016/AIR/Publications/Air_pollution_trends_](http://www.unece.org/fileadmin/DAM/env/documents/2016/AIR/Publications/Air_pollution_trends_in_the_EMEP_region.pdf)
 795 [in_the_EMEP_region.pdf](http://www.unece.org/fileadmin/DAM/env/documents/2016/AIR/Publications/Air_pollution_trends_in_the_EMEP_region.pdf), 2016.
- Colette, A., Andersson, C., Manders, A., Mar, K., Mircea, M., Pay, M.-T., Raffort, V., Tsyro, S., Cuvelier, C., Adani, M., Bessagnet, B.,
 Bergström, R., Briganti, G., Butler, T., Cappelletti, A., Couvidat, F., D'Isidoro, M., Doumbia, T., Fagerli, H., Granier, C., Heyes, C.,
 Klimont, Z., Ojha, N., Otero, N., Schaap, M., Sindelarova, K., Stegehuis, A. I., Roustan, Y., Vautard, R., van Meijgaard, E., Vivanco, M. G.,
 and Wind, P.: EURODELTA-Trends, a multi-model experiment of air quality hindcast in Europe over 1990–2010, Geoscientific Model
 800 Development, 10, 3255–3276, <https://doi.org/10.5194/gmd-10-3255-2017>, <https://www.geosci-model-dev.net/10/3255/2017/>, 2017a.
- Colette, A., Solberg, S., Beauchamp, M., Bessagnet, B., Malherbe, L., Guerreiro, C., and Team, E.-T. M.: Long term air quality trends in
 Europe. Contribution of meteorological variability, natural factors and emissions, Long term air quality trends in EuropeContribution of
 meteorological variability, natural factors and emissions. ETC/ACM Technical Paper 2016/7, European Topic Centre on Air Pollution and
 Climate Change Mitigation (ETC/A, Bilthoven, The Netherlands, [https://www.eionet.europa.eu/etcs/etc-atni/products/etc-atni-reports/](https://www.eionet.europa.eu/etcs/etc-atni/products/etc-atni-reports/etcacm_tp_2016_7_aqtrendseurope)
 805 [etcacm_tp_2016_7_aqtrendseurope](https://www.eionet.europa.eu/etcs/etc-atni/products/etc-atni-reports/etcacm_tp_2016_7_aqtrendseurope), 2017b.
- Colette, A., Solberg, S., Aas, W., and Walker, S.-E.: Understanding Air Quality Trends in Europe, Eionet Report - ETC/ATNI 2020/8,
<https://www.eionet.europa.eu/etcs/etc-atni>, 2021.
- Crippa, M., Janssens-Maenhout, G., Dentener, F., Guizzardi, D., Sindelarova, K., Muntean, M., Van Dingenen, R., and Granier, C.: Forty
 years of improvements in European air quality: regional policy-industry interactions with global impacts, Atmospheric Chemistry and
 810 Physics, 16, 3825–3841, <https://doi.org/10.5194/acp-16-3825-2016>, <https://www.atmos-chem-phys.net/16/3825/2016/>, 2016.
- Cusack, M., Alastuey, A., Pérez, N., Pey, J., and Querol, X.: Trends of particulate matter (PM_{2.5}) and chemical composition at a regional
 background site in the Western Mediterranean over the last nine years (2002–2010), Atmospheric Chemistry and Physics, 12, 8341–8357,
<https://doi.org/10.5194/acp-12-8341-2012>, <https://www.atmos-chem-phys.net/12/8341/2012/>, 2012.
- Dahlgren, P., Landelius, T., Kållberg, P., and Gollvik, S.: A high-resolution regional reanalysis for Europe. Part 1: Three-dimensional re-
 815 analysis with the regional HIGH-Resolution Limited-Area Model (HIRLAM), Quarterly Journal of the Royal Meteorological Society, 142,
 2119–2131, 2016.
- Dee, D. P., Uppala, S. M., Simmons, A., Berrisford, P., Poli, P., Kobayashi, S., Andrae, U., Balmaseda, M., Balsamo, G., Bauer, d. P., et al.:
 The ERA-Interim reanalysis: Configuration and performance of the data assimilation system, Quarterly Journal of the royal meteorological
 society, 137, 553–597, 2011.
- 820 Denier van der Gon, H. A. C., Bergström, R., Fountoukis, C., Johansson, C., Pandis, S. N., Simpson, D., and Visschedijk, A. J. H.: Particulate
 emissions from residential wood combustion in Europe - revised estimates and an evaluation, Atmos. Chem. Physics, 15, 6503–6519,
<https://doi.org/10.5194/acp-15-6503-2015>, <http://www.atmos-chem-phys.net/15/6503/2015/>, 2015.
- EEA: Emissions of primary particles and secondary particulate matter precursors. Last modified 23 Feb 2018, Tech. rep., European Environ-
 ment Agency, <https://www.eea.europa.eu/data-and-maps/indicators/emissions-of-primary-particles-and-1>, 2008.
- 825 Fagerli, H. and Aas, W.: Trends of nitrogen in air and precipitation: Model results and observations at EMEP sites in Europe, 1980–2003,
 Environmental Pollution, 154, 448–461, 2008.
- Guerreiro, C. B., Foltescu, V., and De Leeuw, F.: Air quality status and trends in Europe, Atmospheric environment, 98, 376–384, 2014.



- Jacob, D., Petersen, J., Eggert, B., Alias, A., Christensen, O. B., Bouwer, L. M., Braun, A., Colette, A., Déqué, M., Georgievski, G., et al.: EURO-CORDEX: new high-resolution climate change projections for European impact research, *Regional Environmental Change*, 14, 563–578, 2014.
- Jathar, S. H., Gordon, T. D., Hennigan, C. J., Pye, H. O. T., Pouliot, G., Adams, P. J., Donahue, N. M., and Robinson, A. L.: Unspeciated organic emissions from combustion sources and their influence on the secondary organic aerosol budget in the United States, *Proceedings of the National Academy of Sciences of the United States of America*, 111, 10 473–10 478, <https://doi.org/10.1073/pnas.1323740111>, 2014.
- Kendall, M.: Rank correlation methods (4th edn.) Charles Griffin, San Francisco, CA, 8, 1975.
- Klimont, Z., Höglund-Isaksson, L., Heyes, C., Rafaj, P., Schoepp, W., Cofala, J., Purohit, P., Borken-Kleefeld, J., Kupiainen, K., Kiesewetter, G., et al.: Global scenarios of air pollutants and methane: 1990–2050, 2016.
- Klimont, Z., Kupiainen, K., Heyes, C., Purohit, P., Cofala, J., Rafaj, P., Borken-Kleefeld, J., and Schöpp, W.: Global anthropogenic emissions of particulate matter including black carbon, *Atmospheric Chemistry and Physics*, 17, 8681–8723, <https://doi.org/10.5194/acp-17-8681-2017>, <https://www.atmos-chem-phys.net/17/8681/2017/>, 2017.
- Langner, J., Engardt, M., Baklanov, A., Christensen, J. H., Gauss, M., Geels, C., Hedegaard, G. B., Nuterman, R., Simpson, D., Soares, J., Sofiev, M., Wind, P., and Zakey, A.: A multi-model study of impacts of climate change on surface ozone in Europe, *Atmos. Chem. Phys.*, 12, 10 423–10 440, <https://doi.org/10.5194/acp-12-10423-2012>, <http://www.atmos-chem-phys.net/12/10423/2012/>, 2012.
- Mann, H.: Non-Parametric Tests against Trend. *Econometrica*, 13, 245–259, Mantua, NJ, SR Hare, Y. Zhang, JM Wallace, and RC Francis (1997), A Pacific decadal, 1945.
- Messina, P., Lathiere, J., Sindelarova, K., Vuichard, N., Granier, C., Ghattas, J., Cozic, A., and Hauglustaine, D. A.: Global biogenic volatile organic compound emissions in the ORCHIDEE and MEGAN models and sensitivity to key parameters, *Atmos. Chem. Phys.*, 16, 14 169–14 202, <https://doi.org/10.5194/acp-16-14169-2016>, 2016.
- Mortier, A., Gliß, J., Schulz, M., Aas, W., Andrews, E., Bian, H., Chin, M., Ginoux, P., Hand, J., Holben, B., et al.: Evaluation of climate model aerosol trends with ground-based observations over the last 2 decades—an AeroCom and CMIP6 analysis, *Atmospheric Chemistry and Physics*, 20, 13 355–13 378, 2020.
- Myhre, G., Aas, W., Cherian, R., Collins, W., Faluvegi, G., Flanner, M., Forster, P., Hodnebrog, Ø., Klimont, Z., Lund, M. T., Mülmenstädt, J., Lund Myhre, C., Olivé, D., Prather, M., Quaas, J., Samset, B. H., Schnell, J. L., Schulz, M., Shindell, D., Skeie, R. B., Takemura, T., and Tsyro, S.: Multi-model simulations of aerosol and ozone radiative forcing due to anthropogenic emission changes during the period 1990–2015, *Atmospheric Chemistry and Physics*, 17, 2709–2720, <https://doi.org/10.5194/acp-17-2709-2017>, <https://www.atmos-chem-phys.net/17/2709/2017/>, 2017.
- Ots, R., Young, D. E., Vieno, M., Xu, L., Dunmore, R. E., Allan, J. D., Coe, H., Williams, L. R., Herndon, S. C., Ng, N. L., Hamilton, J. F., Bergström, R., Di Marco, C., Nemitz, E., Mackenzie, I. A., Kuenen, J. J. P., Green, D. C., Reis, S., and Heal, M. R.: Simulating secondary organic aerosol from missing diesel-related intermediate-volatility organic compound emissions during the Clean Air for London (ClearLo) campaign, *Atmos. Chem. Phys.*, 16, 6453–6473, <https://doi.org/10.5194/acp-16-6453-2016>, <http://www.atmos-chem-phys.net/16/6453/2016/>, 2016.
- Platt, S. M., El Haddad, I., Pieber, S. M., Zardini, A. A., Suarez-Bertoa, R., Clairotte, M., Daellenbach, K. R., Huang, R. J., Slowik, J. G., Hellebust, S., Temime-Roussel, B., Marchand, N., de Gouw, J., Jimenez, J. L., Hayes, P. L., Robinson, A. L., Baltensperger, U., Astorga, C., and Prevot, A. S. H.: Gasoline cars produce more carbonaceous particulate matter than modern filter-equipped diesel cars, *SCIENTIFIC REPORTS*, 7, <https://doi.org/10.1038/s41598-017-03714-9>, 2017.



- Schöpp, W., Klimont, Z., Suutari, R., and Cofala, J.: Uncertainty analysis of emission estimates in the RAINS integrated assessment model, *Environmental Science & Policy*, 8, 601–613, 2005.
- Simpson, D. and Denier van der Gon, H.: Problematic emissions - particles or gases?, in: *Transboundary particulate matter, photo-oxidants, acidifying and eutrophying components*. EMEP Status Report 1/2015, pp. 87–96, The Norwegian Meteorological Institute, Oslo, Norway, 2015.
- Simpson, D., Fagerli, H., Colette, A., van der Gon, H. D., Dore, C., Hallquist, M., Hansson, H. C., Maas, R., and Rouil, L. e. a.: How should condensables be included in PM emission inventories reported to EMEP/CLRTAP?, Report of the expert workshop on condensable organics organised by msc-w, gothenburg, 17-19th march 2020., The Norwegian Meteorological Institute, Oslo, Norway.
- Simpson, D., Winiwarter, W., Börjesson, G., Cinderby, S., Ferreira, A., Guenther, A., Hewitt, C. N., Janson, R., Khalil, M. A. K., Owen, S., Pierce, T. E., Puxbaum, H., Shearer, M., Skiba, U., Steinbrecher, R., Tarrasón, L., and Öquist, M. G.: Inventorying emissions from Nature in Europe, *J. Geophys. Res.*, 104, 8113–8152, 1999.
- Simpson, D., Benedictow, A., Berge, H., Bergström, R., Emberson, L., Fagerli, H., Flechard, C., Hayman, G., Gauss, M., Jonson, J., Jenkin, M., Nyíri, A., Richter, C., Semeena, V., Tsyro, S., Tuovinen, J.-P., Valdebenito, A., and Wind, P.: The EMEP MSC-W chemical transport model – technical description, *acp*, 12, 7825–7865, <https://doi.org/10.5194/acp-12-7825-2012>, 2012.
- Skamarock, W. C., Klemp, J. B., Dudhia, J., Gill, D. O., Barker, D. M., Wang, W., and Powers, J. G.: A description of the advanced research WRF version 2, Tech. rep., National Center For Atmospheric Research Boulder Co Mesoscale and Microscale . . . , 2005.
- Solberg, S., Jonson, J., Horalek, J., Larssen, S., and De Leeuw, F.: Assessment of ground-level ozone in EEA member countries, with a focus on long-term trends, EEA Report No7/2009, European Environment Agency, Copenhagen, 2009.
- Spracklen, D. V., Arnold, S. R., Sciare, J., Carslaw, K. S., and Pio, C.: Globally significant oceanic source of organic carbon aerosol, *Geophys. Res. Lett.*, 35, <https://doi.org/10.1029/2008GL033359>, 2008.
- Steghuis, A., Vautard, R., Ciais, P., Teuling, A., Miralles, D., and Wild, M.: An observation-constrained multi-physics WRF ensemble for simulating European mega heat waves, *Geoscientific Model Development*, 8, 2285–2298, 2015.
- Terrenoire, E., Bassagnet, B., Rouil, L., Tognet, F., Pirovano, G., Letinois, L., Beauchamp, M., Colette, A., Thunis, P., Amann, M., et al.: High-resolution air quality simulation over Europe with the chemistry transport model CHIMERE, *Geoscientific Model Development*, 8, 21–42, 2015.
- Theobald, M. R., Vivanco, M. G., Aas, W., Andersson, C., Ciarelli, G., Couvidat, F., Cuvelier, K., Manders, A., Mircea, M., Pay, M.-T., Tsyro, S., Adani, M., Bergström, R., Bessagnet, B., Briganti, G., Cappelletti, A., D’Isidoro, M., Fagerli, H., Mar, K., Otero, N., Raffort, V., Roustan, Y., Schaap, M., Wind, P., and Colette, A.: An evaluation of European nitrogen and sulfur wet deposition and their trends estimated by six chemistry transport models for the period 1990–2010, *Atmospheric Chemistry and Physics*, 19, 379–405, <https://doi.org/10.5194/acp-19-379-2019>, <https://www.atmos-chem-phys.net/19/379/2019/>, 2019.
- Tørseth, K., Aas, W., Breivik, K., Fjæraa, A. M., Fiebig, M., Hjellbrekke, A.-G., Lund Myhre, C., Solberg, S., and Yttri, K. E.: Introduction to the European Monitoring and Evaluation Programme (EMEP) and observed atmospheric composition change during 1972–2009, *Atmospheric Chemistry and Physics*, 12, 5447–5481, 2012.
- UNECE: HANDBOOK FOR THE 1979 CONVENTION ON LONG-RANGE TRANSBOUNDARY AIR POLLUTION AND ITS PROTOCOLS, UNECE Convention on Long-range Transboundary Air Pollution, UNITED NATIONS, New York and Geneva, 2004, joint WHO/Convention Task Force on the Health Aspects of Air Pollution, 2004.



- Van Donkelaar, A., Martin, R. V., Brauer, M., and Boys, B. L.: Use of satellite observations for long-term exposure assessment of global concentrations of fine particulate matter, *Environmental health perspectives*, 123, 135–143, <https://doi.org/10.1289/ehp.1408646>, 2015.
- 905 Van Meijgaard, E., Van Ulft, L., Lenderink, G., De Roode, S., Wipfler, E. L., Boers, R., and van Timmermans, R.: Refinement and application of a regional atmospheric model for climate scenario calculations of Western Europe, KVR 054/12, KVR, 2012.
- Winiwarter, W., Bauer, H., Caseiro, A., and Puxbaum, H.: Quantifying emissions of primary biological aerosol particle mass in Europe, *Atmos. Environ.*, 43, 1403–1409, <https://doi.org/10.1016/j.atmosenv.2008.01.037>, 2009.
- Yttri, K. E., Simpson, D., Nøjgaard, J. K., Kristensen, K., Genberg, J., Stenström, K., Swietlicki, E., Hillamo, R., Aurela, M., Bauer, H.,
910 Offenberg, J. H., Jaoui, M., Dye, C., Eckhardt, S., Burkhardt, J. F., Stohl, A., and Glasius, M.: Source apportionment of the summer time carbonaceous aerosol at Nordic rural background sites, *Atmos. Chem. Phys.*, 11, 13 339–13 357, <https://doi.org/10.5194/acp-11-13339-2011>, <http://www.atmos-chem-phys.net/11/13339/2011/>, 2011.